A Study of a Hamiltonian Model for Martensitic Phase Transformations Including Microkinetic Energy

FLORIAN THEIL
University of Oxford, Mathematical Institute 24–29 St. Giles, Oxford OX1 3LB, UK

VALERY I. LEVITAS
Department of Mechanical Engineering, Texas Tech University, Lubbock, Texas 79409-1021, USA

(Received 1 December 1998; Final version 29 June 1999)

Abstract: How can a system in a macroscopically stable state explore energetically more favorable states, which are far away from the current equilibrium state? Based on continuum mechanical considerations, the authors derive a BOUSSINESQ-type equation

$$\rho\ddot{u} = \partial_x\sigma(\partial_x u) + \beta\partial_x^2\ddot{u}, \quad x \in (0,1),\ \beta > 0,$$

which models the dynamics of martensitic phase transformations. Here $\rho > 0$ is the mass density, $\beta\partial_x^2\ddot{u}$ is a regularization term which models the inertial forces of oscillations within a representative volume of length $\sqrt{\beta}$, and σ is a nonmonotone stress-strain relation. The solutions of the system, which the authors refer to as the *microkinetically* regularized wave equation, exhibit strong oscillations after times of order $\sqrt{\beta}$ and relaxation of spatial averages can be confirmed. This means that macroscopic fluctuations of the solutions decay, to the benefit of microscopic fluctuations. From the macroscopic point of view, this can be interpreted as a transformation of macroscopic kinetic energy into heat, i.e., as energy dissipation (despite the fact the authors consider a conservative system). The mathematical analysis for the microkinetically regularized wave equation consists in two parts. First, the authors present some analytical and numerical results on the propagation of phase boundaries and relaxation effects. Despite the fact that the model is conservative, it exhibits hysteretic behavior. Such behavior is usually interpreted in macroscopic models in terms of a dissipative threshold which the driving force must overcome to ensure that the phase transformation proceeds. The threshold value depends on the volume of the transformed phase as observed in known experiments. Second, the authors investigate the dynamics of oscillatory solutions. Their mathematical tools are Young measures, which describe the one-point statistics of the fluctuations. They present a formalism which allows them to describe the effective dynamics of rapidly fluctuating solutions. The extended system has nontrivial equilibria which are only visible when oscillatory solutions are considered. The new method enables them to derive a numerical scheme for oscillatory solutions based on particle methods.

Key Words: Phase transformations, oscillations, Young measures, Hamiltonian dynamics, nonlinear partial differential equations

1. INTRODUCTION

In this work, we study the onset and propagation of oscillations in a model for martensitic phase transformations. Consider the simple tension of a rod of nonlinear elastic material

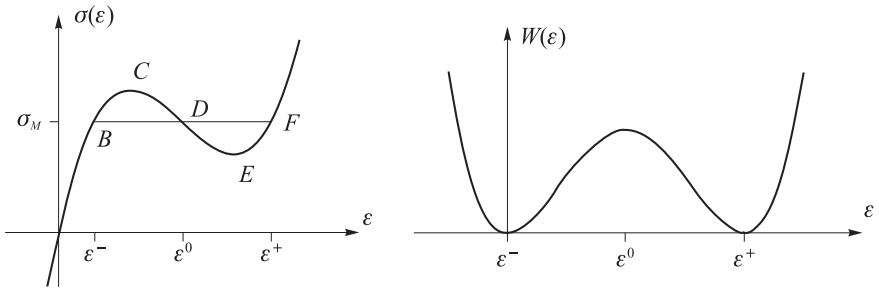

Figure 1. Nonmonotone stress strain relation and nonconvex elastic energy.

with a graph $\sigma = \sigma(\varepsilon)$, shown in Figure 1, where σ and ε are tensile stress and strain, respectively. The graph shown in Figure 1 corresponds to a nonconvex free energy $W(\varepsilon)$, and is typical for materials with martensitic phase transformations (PT). We will label the phases corresponding to the branches *BC* and *EF* (-) and (+), respectively; branch *CDE* exhibits an unstable intermediate state. The principle of minimum free energy for such materials results in the formation of a phase mixture and a macroscopic deformation along the line *BDF* at constant stress σ_M (Maxwell line), rather than along the lines *BCDEF*. Considering a quasi-static experiment at some stress σ_0, a macroscopic portion of the material is deformed from ε^- to ε^+. At the next total strain increment $\Delta\varepsilon$, the next portion of material undergoes PT. During the whole process of PT, the strains in the phases (-) and (+) are fixed and equal to ε^- and ε^+, the stress is constant $\sigma = \sigma_0$, and $\Delta\varepsilon$ is related to the increment Δc of the volume fraction of a new phase.

It is clear that in quasi-static treatments, we do not follow the original stress-strain curve $\varepsilon \to \sigma(\varepsilon)$ but, rather, introduce a strain jump from ε^- to ε^+ at constant stress for each transforming particle. To be consistent with the original stress-strain relation, the concept of fluctuating stresses was introduced in [1, 2]. Fluctuating stress σ_{fluct} is defined as $\sigma_{\text{fluct}} = \sigma(\varepsilon) - \sigma_M$ in the interval $[\varepsilon^-, \varepsilon^+]$: it varies in accordance with the line *BCDEF*, relative to the line *BDF*. This fluctuating stress overcomes the energy barrier *BCD*, but due to the very small time interval of its action, it is not taken into account in the continuum relations. In the equilibrium process, the time averaged value of σ_{fluct} is equal to zero.

This concept is useful for the development of some kinetic models [1, 2] which only use some important properties of the stress-strain curve $\sigma = \sigma(\varepsilon)$ but not the precise course of the unstable part.

One of the main unsolved problems is to find a proper physical model for fluctuations and to include it in the continuum description of PT. One possibility is to take into account microinertia in constitutive equations, i.e., to consider a constitutive equation

$$\sigma_m = \sigma(\varepsilon) + \beta\ddot{\varepsilon}, \tag{1.1}$$

where σ_m is the macroscopic stress. The constitutive assumption (1.1) and the conservation of linear momentum lead us to the following evolution equation:

$$\rho\ddot{u} = \partial_x(\sigma(\partial_x u) + \beta\partial_x\ddot{u}), \quad x \in (0,1),\ \rho \geq 0,\ \beta > 0, \tag{1.2}$$

where $u : \mathbb{R}^+ \times \Omega \to \mathbb{R}$ is the deformation of an elastic body $\Omega = (0,1) \subset \mathbb{R}$ at time t and ρ is the mass density. The coefficient β describes the inertia of microscopic fluctuations: for a derivation, see Section 2. For reasons which will become clear there, we will refer to system (1.2) as the *microkinetically* regularized wave equation. If appropriate boundary conditions are imposed, the generalized energy $\int_0^1 (\frac{\rho}{2}\dot{u}^2 + W(\partial_x u) + \frac{\beta}{2}(\partial_x \dot{u})^2)\mathrm{d}x$ is conserved. The aim of this paper is to present the first mathematical results for such a model.

Equation (1.2) constitutes a well-posed Cauchy problem. In the following section, we present a continuum mechanical derivation of the microkinetically regularized wave equation, based on an approach developed in [3, 4, 5] to describe the dynamics of phase transformations. Since in this derivation finite wavelengths are assumed, it is not possible to show that (1.2) approximates the phase transformation problem if the strain oscillates at a wavelength of order $\sqrt{\beta}$. However, the obviously very interesting behavior of the solutions motivates us to analyze the dynamics of oscillations with modern mathematical tools like Young measures. Many of our results are also valid for the improved Boussinesq equation:improved Boussinesq equation

$$\ddot{u} = u_{xx} + (u^p)_{xx} + \ddot{u}_{xx} .$$

(See Section 2 for references.)

In Section 3, important phenomena of the dynamics are investigated numerically and analytically. We show that the system possesses solitary wave solutions. In the numerical simulations, quasi-dissipative behavior can be observed. Due to the nonmonotonicity of σ, the solutions exhibit high- frequency oscillations in space after times which are proportional to $\sqrt{\beta}$, even if the initial state is smooth. These spatial fluctuations can be interpreted as heat. The introductory problem motivates the development of mathematical tools which simplify the study of oscillatory solutions. We expect that the results will be useful for future work. We find a critical threshold value for the minimal driving force of the transformation process. The threshold value depends on the amount of transformed energy.

There exists a rich literature concerning regularizations of quasilinear wave-equations with nonmonotone stress-strain relation, see, e.g., [6] and the references therein. The problem lies in the ill-posedness of the Cauchy problem for the quasilinear wave-equation $\rho\ddot{u} = \partial_x \sigma(\partial_x u)$. The hope is that the regularization selects the physically correct solution if the strength of the regularization tends to 0. Another approach consists of the assumption of a kinetic relation to determine the velocity of a moving phase boundary. Using this additional constitutive law, one can show that the Riemann problem has a unique solution (see [7, 8]). Indeed, the solutions of the Riemann problem with viscosity and Van-der-Waals forces generate the kinetic relation, [9].

We are not so much interested in the singular limit $\beta \to 0$, but more in the qualitative behavior of the solutions if β is nonzero. The system distinguishes in a natural way between two different scales (microscale and macroscale). This phenomenon allows us to characterize the dynamics of the microstructure in a unique fashion. To this end, we introduce the notion of Young measures, which can be viewed as generalized limits of sequences of highly oscillatory functions. One major disadvantage of Young measures is that they do not work well together with pseudo differential operators of degree 0 like the Helmholtz projection, which maps a vector field onto the gradient part. But this is essential if space dimensions greater than one are considered. Therefore, the analysis is restricted to the one- dimensional case.

Young measures have been used successfully for phase transformation problems. In [10], they are applied to the three-dimensional crystallographic theory. Fundamental results on oscillatory solutions to dynamical problems have been obtained by Tartar in [11, 12, 13]. Using methods from calculus of variations, Kinderlehrer and Pedregal [14] showed that dynamical models for phase transformations admit Young measure solutions. The approach outlined in this work has been applied before to the viscoelastic system with nonmonotone stress-strain relation $\rho\ddot{u} = \partial_x(\sigma(\partial_x u) + \beta\partial_x \dot{u})$ (see [15]).

The mathematical analysis for oscillatory solutions of the microkinetic model consists of two parts: short-time behavior and long-time behavior.

In Section 4, we derive an effective equation for Young-measure solutions. These generalized solutions are unique and they approximate the dynamics of highly oscillatory solutions over finite times. This approach can be viewed as an analogy to homogenization theory. There the aim is the derivation of a macroscopic law when the material properties are oscillatory. In our case, it turns out that the dynamics of oscillatory solutions can be reduced to a transport equation which has structural similarity to the Vlasov-Poisson system. The Vlasov-Poisson system describes the evolution of electrically charged plasmas (see, e.g., [16]).

The microkinetic system exhibits some kind of ergodic behavior. Even if we start with a smooth initial condition, the solutions soon become oscillatory (cf. Fig. 2). Especially in the region $x \in [0.1, 0.2]$, the solution looks very much like a Young measure.

In Section 5, we demonstrate that the extended system has a large number or equilibria which are not generalized limits of sequences of stationary solutions of (1.2). The physical interpretation of this result is as follows. Despite the very dynamical oscillatory behavior of each material point, macroscopic statistical characteristics, like volume fraction of new phase, are stationary for equilibrium solutions of the extended system. Thus, Young measures are an important concept for finding macroscopic information using nonstationary oscillatory solutions. This observation has been made earlier for the equations of ideal incompressible magneto hydrodynamics (see [17, 18]). There, the authors analyze so- called relaxed equilibrium states, which correspond to highly oscillatory nonstationary solutions of the evolution equations.

If we consider the nonphysical limit $\rho \to 0$, it can be shown that almost every solution tends to a stationary Young measure as time goes to infinity. This is a genuinely infinite dimensional result since the system is Hamiltonian. In finite dimensional Hamiltonian systems, the phase-space volume is conserved, thus generic solutions do not converge to an equilibrium.

In [15], the long-time behavior of oscillatory solutions has been investigated for the viscoelastically damped system. There it is found that the microstructure region shrinks when t tends to infinity. This contrasts with the microkinetic system, where microstructure can be generated in the long-time limit.

The convergence toward an equilibrium Young measure is a special case of *relaxation of spatial averages* which is a synonym for the more mathematical notion of weak convergence, i.e., energy which is at the beginning only visible at the macroscopic level is transformed into microscopic fluctuations. Hence on the macroscopic level the solution becomes stationary. This behavior does not correspond to the numerical results of E. Fermi, J. Pasta, and S. Ulam [19] where a discretized nonlinear wave equation

$$\rho\ddot{\varepsilon}_i = \sigma(\varepsilon_{i+1}) - \sigma(\varepsilon_{i-1})$$

is investigated. They observed a recurrence phenomenon, i.e., after fixed time intervals the solution returns very close to the initial deformation.

The study of the microkinetic system is concluded by a systematic numerical investigation of the relaxation behavior in the case $\rho > 0$. In Section 6, a numerical scheme based on particle methods is developed and simulation results concerning the long-time behavior of solutions for values of ρ greater than 0 are presented. It turns out that the spatial coupling due to the nonvanishing of ρ complicates the long-time behavior considerably. The solutions develop microstructure, but there are no indications that the solutions tend toward a stationary Young measure if $\rho > 0$. However, a major portion of the initial macroscopic kinetic energy is transformed into microscopic fluctuations.

2. CONSTITUTIVE EQUATION FOR MATERIAL WITH MICROSCOPIC INERTIA

For a formal derivation of the constitutive equation, we consider the d-dimensional setting, $d = 1, 2, 3$, although the subsequent analysis is restricted to the one-dimensional case. For simplicity, geometrically linear elasticity theory is used. However, we insist that the derivation is completely analogous if geometrically nonlinear theory is used. In this case, we can use the deformation gradient and the first nonsymmetric Piola-Kirchhoff stress tensor as conjugate variables. For the convenience of readers who are not familiar with the notations in continuum mechanics, we repeat the basic definitions. Let $\Omega \subset \mathbb{R}^d$ be the reference configuration of an elastically deformable body. The superscript t denotes transposition, and ∇ is the gradient operator. We use bold letters to indicate tensors and vectors, the coefficients are written with normal letters. The dot " $\cdot$ " and the colon " : " denote contraction of tensors over one and two indices, respectively: $(\mathbf{A}\cdot\mathbf{B})_{ik} = \sum_j A_{ij} B_{jk} = A_{ij} B_{jk}$ and $\mathbf{A} : \mathbf{B} = \mathrm{tr}(\mathbf{A} \cdot \mathbf{B}^t) = A_{ij} B_{ij}$, where Einstein's summation convention is adopted for the last identities. By $\mathbf{A} \otimes \mathbf{B}$ we denote the fourth-order tensor with components $(A_{ij} B_{kl})$.

Let us consider a representative volume $\omega \subset \Omega$ of the microheterogeneous material bounded by a surface $\partial\omega$, with unit normal vector $\mathbf{n}$. We assume that ω is much smaller than Ω and that the center of mass is located at the origin. Let $\mathbf{r}$ be the particle position and $\mathbf{u}$ the continuous displacement field, i.e., for every material point $\mathbf{r}$ in the reference configuration, the position at time t is given by $\widetilde{\mathbf{u}}(t, \mathbf{r})$. By $\widetilde{\boldsymbol{\sigma}}$ we denote the stress tensor and $\widetilde{\boldsymbol{\varepsilon}} = \nabla\widetilde{\mathbf{u}}$ is the deformation gradient tensor. Here $\widetilde{}$ means that the local values of the parameters are used as opposed to their macroscopic counterparts. Let us introduce, in the usual way, the macroscopic stress σ_m and deformation gradient ε_m tensors,

$$\boldsymbol{\sigma}_m^t = \mathrm{vol}(\omega)^{-1} \int_{\partial\omega} \mathbf{r} \otimes \widetilde{\boldsymbol{\sigma}}\cdot\mathbf{n}\mathrm{d}S; \qquad \boldsymbol{\varepsilon}_m = \mathrm{vol}(\omega)^{-1} \int_{\partial\omega} \widetilde{\mathbf{u}} \otimes \mathbf{n}\mathrm{d}S. \tag{2.1}$$

The macroscopic stress tensor is the critical quantity which allows one to analyze the macroscopic behavior. Definition (2.1) can be motivated as follows. Let E_ω be the total

energy contained in the representative volume. Then the power of the external forces can be computed using the formula

$$\frac{\mathrm{d}}{\mathrm{d}t}E_\omega = \int\limits_{\partial\omega} \left(\widetilde{\boldsymbol{\sigma}}^t \cdot \dot{\widetilde{\mathbf{u}}}\right) \cdot \mathbf{n}\mathrm{d}S. \tag{2.2}$$

Assuming that the velocity distribution corresponds to a macroscopically homogeneous deformation on the boundary, we find that $\dot{\widetilde{\mathbf{u}}}(\mathbf{r}) = \dot{\mathbf{u}}_0 + \dot{\boldsymbol{\varepsilon}}_m \cdot \mathbf{r}$ holds for all $\mathbf{r} \in \partial\omega$. Substituting this Ansatz into (2.2), one finds that

$$\begin{aligned}
\frac{\mathrm{d}}{\mathrm{d}t}E_\omega &= \int\limits_{\partial\omega} (\widetilde{\boldsymbol{\sigma}}^t \cdot (\dot{\boldsymbol{\varepsilon}}_m \cdot \mathbf{r})) \cdot \mathbf{n}\mathrm{d}S + \int\limits_{\partial\omega} (\widetilde{\boldsymbol{\sigma}} \cdot \mathbf{n}) \cdot \dot{\mathbf{u}}_0 \mathrm{d}S \\
&= \dot{\boldsymbol{\varepsilon}}_m^t : \int\limits_{\partial\omega} \mathbf{r} \otimes \widetilde{\boldsymbol{\sigma}} \cdot \mathbf{n}\mathrm{d}S + \dot{\mathbf{u}}_0 \cdot \int\limits_{\partial\omega} (\widetilde{\boldsymbol{\sigma}} \cdot \mathbf{n})\mathrm{d}S \\
&= \mathrm{vol}(\omega) \cdot \dot{\boldsymbol{\varepsilon}}_m : \boldsymbol{\sigma}_m + \dot{\mathbf{u}}_0 \cdot \mathbf{F}_m ,
\end{aligned}$$

where $\mathbf{F}_m = \int_{\partial\omega} (\widetilde{\boldsymbol{\sigma}} \cdot \mathbf{n})\mathrm{d}S$ is the macroscopic force. Thus, in absence of macroscopic translations, the power of the external stresses, through which the representative volume interacts with the neighborhood, is equal to $\boldsymbol{\sigma}_m : \dot{\boldsymbol{\varepsilon}}_m$, as for material points. The symmetry of the stress tensor in the geometrically linear theory corresponds to the symmetry of the Cauchy stress tensor in the geometrically nonlinear theory. In both theories, the macroscopic stress tensor is not symmetric in general: it is possible to transfer energy by rotations. The macroscopic forces will be neglected in the further considerations. Using the Gauss theorem and the equations of motion without body forces,

$$\nabla \cdot \widetilde{\boldsymbol{\sigma}} = \widetilde{\rho}\ddot{\mathbf{u}}, \tag{2.3}$$

where $\widetilde{\rho}$ is the mass density, we obtain from eqs. (2.1) and (2.3)

$$\boldsymbol{\sigma}_m = \langle \widetilde{\boldsymbol{\sigma}} \rangle + \langle \widetilde{\rho}\ddot{\mathbf{u}} \otimes \mathbf{r} \rangle; \qquad \boldsymbol{\varepsilon}_m = \langle \widetilde{\boldsymbol{\varepsilon}} \rangle, \tag{2.4}$$

where $\langle ... \rangle = \mathrm{vol}(\omega)^{-1} \int_\omega (...)\mathrm{d}x$ is the average over the volume ω. When the macroscopic stress tensor is approximated by the averaged stress tensor, the resulting errors can be expressed as accelerations or inertial stresses. The averaged value $\langle \widetilde{\boldsymbol{\sigma}} \rangle$ neglects rapid oscillations in the interior of the representative volume. The kinetic energy of these oscillations is responsible for the inertial stresses. It is crucial that the inertial stresses have a regularizing effect. They enlarge the inertia of the material in such a way that a well-posed Cauchy problem can be derived even if for the averaged stress tensor a nonmonotone dependency of the macroscopic deformation gradient $\boldsymbol{\varepsilon}_m$ is assumed.

If the diameter of ω tends to 0, then the second term in (2.4) vanishes and

$$\boldsymbol{\sigma}_m = \langle \widetilde{\boldsymbol{\sigma}} \rangle, \tag{2.5}$$

i.e., the macroscopic stress σ_m is equal to microscopic stresses averaged over the infinitesimal volume $\boldsymbol{\sigma}_v := \langle \widetilde{\boldsymbol{\sigma}} \rangle$. The same holds if the body is in an equilibrium state. The next step

consists of prescribing the constitutive equations for $\widetilde{\boldsymbol{\sigma}}$ (in the micromechanical approach) or directly for $\boldsymbol{\sigma}_v$ at the phenomenological level. To describe martensitic PT in elastic material, a nonconvex elastic potential is used, which results in a nonmonotone stress-strain relation $\boldsymbol{\sigma}_v = \mathbf{f}(\boldsymbol{\varepsilon}_m)$. Due to the ill posedness of the dynamic boundary-value problem for this type of materials, a number of mathematical and physical regularization methods have been suggested. One of them consists of the introduction of viscosity, i.e., one considers a viscoelastic material. In this paper, we would like to limit ourselves to nondissipative materials. Another approach is related to the introduction of a characteristic material size, e.g., by introduction of higher strain gradients $\nabla\boldsymbol{\varepsilon}_m, \nabla\nabla\boldsymbol{\varepsilon}_m, \ldots$ or nonlocal stress-strain relations. As it is shown in [1], in a framework of micromechanical consideration, the macroscopic deformation gradient $\mathbf{B}$ and the work-conjugated third-order tensors of the hyperstress $\mathbf{M}$ can be defined by the formulas

$$\mathbf{B} = \mathrm{vol}(\omega)^{-1} \int\limits_{\partial\omega} \widetilde{\boldsymbol{\varepsilon}} \otimes \mathbf{n} \mathrm{d}S; \qquad \mathbf{M} = \frac{\mathrm{vol}(\omega)^{-1}}{2} \int\limits_{\partial\omega} \mathbf{r} \otimes \mathbf{r} \otimes \widetilde{\boldsymbol{\sigma}} \cdot \mathbf{n} \mathrm{d}S. \tag{2.6}$$

With the help of the Gauss theorem and the equations of motion for the static case, we obtain

$$\mathbf{B} = \langle \nabla\nabla\mathbf{u} \rangle = \langle \nabla\widetilde{\boldsymbol{\varepsilon}} \rangle; \qquad \mathbf{M} = \langle \mathbf{r} \otimes \widetilde{\boldsymbol{\sigma}} \rangle. \tag{2.7}$$

The tensor $\mathbf{M}$ is nonzero only if the diameter of the representative volume ω is finite. This follows from equation $(2.7)_2$ by considering the limit $\mathrm{diam}(\omega) \to 0$. For macroscopically homogeneous strains $\mathbf{u} = \mathbf{u}_0 + \boldsymbol{\varepsilon}_m \cdot \mathbf{r}$ on $\partial\omega$, we have $\widetilde{\boldsymbol{\varepsilon}} = \boldsymbol{\varepsilon}_m$ on the surface $\partial\omega$, and according to equation (2.6), $\mathbf{B} = \mathbf{0}$. If the macroscopic stresses on $\partial\omega$ are homogeneous, $\widetilde{\boldsymbol{\sigma}} \cdot \mathbf{n} = \boldsymbol{\sigma}_m \cdot \mathbf{n}$ holds and, according to equation (2.7), $\mathbf{M} = \mathbf{0}$ (using $\langle \mathbf{r} \rangle = 0$). Consequently, the tensors $\mathbf{B}$ and $\mathbf{M}$ characterize the heterogeneous distribution of strains and stresses inside the representative volume. Both vanish for macroscopically homogeneous conditions, even if the representative volume is finite.

At the same time, for finite representative volume, the inertial stresses $\boldsymbol{\sigma}_i := \langle \widetilde{\rho}\mathbf{r} \otimes \ddot{\mathbf{u}} \rangle$ are nonzero even for macroscopically homogeneous stress state provided that the accelerations $\ddot{\mathbf{u}}$ are large. As PT represents a highly dynamic process, the contribution of inertial stresses can, in fact, be very important for finite representative volume.

Our next aim is to approximate the compact integral operator $\langle \rho\mathbf{r} \otimes \ddot{\mathbf{u}} \rangle$ by an unbounded differential operator. Expanding $\ddot{\widetilde{\mathbf{u}}}$ around $\mathbf{0}$ to the first order, we have $\ddot{\widetilde{\mathbf{u}}}(\mathbf{r}) = \ddot{\widetilde{\mathbf{u}}}(\mathbf{0}) + \ddot{\widetilde{\boldsymbol{\varepsilon}}}(\mathbf{0}) \cdot \mathbf{r} + \mathcal{O}(\mathrm{diam}(\omega)^2 \|\nabla^2 \ddot{\widetilde{\mathbf{u}}}\|_{L^\infty(\Omega)})$. Thus,

$$\begin{aligned}
\left\langle \rho\mathbf{r} \otimes \ddot{\widetilde{\mathbf{u}}}(t,\cdot) \right\rangle_{ij} &= \tfrac{\rho}{\mathrm{vol}(\omega)} \left\{ \underbrace{\int\limits_{\omega} x_i \ddot{u}_j(\mathbf{0}) \mathrm{d}x}_{=0} + \sum_{k=1}^{d} \int\limits_{\omega} \ddot{\widetilde{\varepsilon}}_{jk}(t,\mathbf{0}) x_i x_k \mathrm{d}x \right\} \\
&+ \mathcal{O}(\mathrm{diam}(\omega)^3 \|\nabla^2 \ddot{\widetilde{\mathbf{u}}}\|_{L^\infty(\Omega)}) \\
&= \rho \sum_{k=1}^{d} \ddot{\widetilde{\varepsilon}}_{jk}(t,\mathbf{0}) \tfrac{1}{\mathrm{vol}(\omega)} \int\limits_{\omega} x_i x_k \mathrm{d}x + \mathcal{O}(\mathrm{diam}(\omega)^3 \|\nabla^2 \ddot{\widetilde{\mathbf{u}}}\|_{L^\infty(\Omega)}).
\end{aligned}$$

Due to the linearity of the integral operator, the estimates are stable under weak convergence, i.e., we may replace $\widetilde{\boldsymbol{\varepsilon}}$ by $\boldsymbol{\varepsilon}_m$. On dropping the error term, we obtain

$$\boldsymbol{\sigma}_m = \boldsymbol{\sigma}_v + \langle \widetilde{\rho}\mathbf{r} \otimes \mathbf{r} \rangle \cdot \ddot{\boldsymbol{\varepsilon}}_m . \tag{2.8}$$

It is clear that the approximation loses validity if the oscillations of $\ddot{\boldsymbol{\varepsilon}}_m$ occur on a length scale of order $\mathrm{diam}(\omega)^3$.

The final step in our derivation consists of taking equation (2.4) as a definition for $\widetilde{\boldsymbol{\sigma}}_m$. This introduces a correction term, which ensures that the averaged stress contains enough information to predict the macroscopic dynamics. This new stress is conservative and related to the acceleration, so we refer to it as microinertial stress. It has a similar effect to viscoelastic damping, namely, the regularization of the velocity.

For one-dimensional tension, when only tensile stress σ and strain ε are important, equation (2.8) results in

$$\sigma_m = \sigma_v + \beta\ddot{\varepsilon}; \qquad \beta = \langle \rho r^2 \rangle , \tag{2.9}$$

where the coefficient β characterizes the inertia of the representative volume at the fixed center of mass, i.e., microscopic inertia. Equation (2.9) resembles a Lagrange equation in the mechanics of discrete systems, with the generalized coordinate ε under the action of external σ_m and conservative σ_v generalized forces. For this reason, we will call the kinetic energy of the representative volume $\frac{1}{2}\beta\dot{\varepsilon}^2$ *microkinetic* energy. If the representative volume is a cube with side length $2a$ and the mass density is homogeneous, then $\beta = \frac{\rho}{3}a^2$.

Equation (1.2) has been derived in the case $\sigma(\varepsilon) = E\varepsilon$ (E is the Young modulus) to describe longitudinal waves in a slender elastic rod [20, p. 428]. The equation is known as Love's modified wave equation. The inertia of radial deformations is taken into account; this allows one, in contrast to the classical one-dimensional wave equation, to describe wave propagation problems in rods where the size of the diameter is comparable to the wavelength. In the case $\sigma(\varepsilon) = \varepsilon + \varepsilon^p, p = 2$, the equation is known as the improved Boussinesq equation. It has been derived in [21] to describe ion-sound waves. The classical Boussinesq equation

$$\ddot{u} = \partial_x^2(u + u^2 + \partial_x^2 u), \tag{2.10}$$

which was derived in 1872 to describe shallow water waves [22], has the shortcoming that the Cauchy problem is ill posed. Thus, it cannot be used to analyze wave propagation problems numerically. The dispersion relations of both Boussinesq equations

$$\begin{aligned} \omega^2 &= k^2(1-k^2) \quad \text{(classical)}, \\ \omega^2 &= k^2(1+k^2)^{-1} \quad \text{(improved)}. \end{aligned}$$

are equivalent to the fourth order for $|k| \ll 1$, which motivates the nomenclature. We will focus on the short wave-length limit $|k| \to \infty$. In this limit, the improved and the classical Boussinesq equation are not related.

For odd numbers p, the mapping $\varepsilon \to \sigma(\varepsilon)$ is monotone; for even numbers, the solutions can blow up in finite times (see, e.g., [23]). We are interested in the case that σ is nonmonotone but the stored elastic energy function $W(W' = \sigma)$ is coercive, i.e., $W(\varepsilon) \to \infty$ as $\varepsilon \to \infty$. To our best knowledge, this case has not been studied in the literature yet.

The microkinetic energy corresponds to the energy of transversal motions in Rayleigh's theory of rods or the virtual kinetic energy of the bubbles in the mechanics of multiphase fluid (e.g., Caflisch). The microkinetic term was also used by Rosenau [24] for a continuum approximation of lattice vibrations. Note that an inertial term in stress-strain relations was introduced and made consistent with thermodynamics in [3, 4]. Earlier, Valanis [25] suggested an inertial contribution in constitutive equations for internal variables, and a way to satisfy the second law of thermodynamics in this case. A general theory, which includes generalized inertial forces for each thermodynamic variable, was developed in [3, 4]. It was shown that in particular cases, thermodynamic inertial forces were well-known for thermal conductivity, moisture propagation in a colloid capillary body, and turbulent transfer, but the equations were not consistent with the second law of thermodynamics.

3. FIRST DISCUSSION OF THE EQUATIONS OF MOTION, SOLITARY WAVES

In this section, we state the precise evolution equations and explain their central properties. To motivate the consideration of oscillatory solutions, simulation results of special solutions are presented.

We set $\Omega = (0,1) \subset \mathbb{R}$. Using the constitutive equation (2.9), where the subscript of σ_m is dropped, we obtain the following nonlinear partial differential equation, which governs the time evolution of u:

$$\begin{aligned} \rho\ddot{u} &= \partial_x(\sigma(\partial_x u) + \beta\partial_x\ddot{u}), \qquad \beta > 0, \rho \geq 0, \\ u|_{t=0} &= u_0,\ \dot{u}|_{t=0} = v_0 \qquad \text{(initial conditions)}, \\ u|_{x=0} &= 0,\ (\sigma(\partial_x u) + \beta\partial_x\ddot{u})|_{x=1} = 0 \qquad \text{(Neumann boundary condition)}. \end{aligned} \tag{3.1}$$

The chosen boundary conditions model an experiment where the rod is free at the right boundary and fixed at the left boundary to exclude translations.

We assume that $\sigma(\cdot)$ is a nonmonotone function with three zeros $\varepsilon^- < \varepsilon^0 < \varepsilon^+$, which satisfies $\lim_{|\varepsilon|\to\infty} \varepsilon \cdot \sigma(\varepsilon) = \infty$. For mathematical simplicity, we do not consider boundary forces to control the experiment. Instead, the shape of the mapping $\varepsilon \mapsto \sigma(\varepsilon)$ is varied with a scalar parameter μ to stabilize or to destabilize a certain phase. Therefore, no assumption that $\int_{\varepsilon^-}^{\varepsilon^+} \sigma(\varepsilon)\mathrm{d}\varepsilon = 0$ is made. The nonconvex function $W(\varepsilon) = \int_0^\varepsilon \sigma(\gamma)\mathrm{d}\gamma$ is usually called double-well potential, the two local minima corresponding to two different phases which are stable with respect to small perturbations. Global existence and uniqueness of solutions to (3.1) is clear, although a formal proof is not provided in this work.

If $\beta = 0$, system (3.1) describes the purely elastic behavior of the rod where no microkinetic forces are taken into account. It is clear that the initial-boundary value problem is well posed only if σ is monotone and so equation (3.1) is hyperbolic. By assuming a nonmonotone stress-strain relation, we have introduced a Hadamard-instability which causes the solutions to start oscillating heavily and blow up in finite time. The term $\beta\partial_x^2\ddot{u}$ is of higher order; thus, for $\beta > 0$ global existence and uniqueness of solutions can be established.

System (3.1) is the evolution equation associated with a Hamiltonian system. The Hamiltonian (energy) which is conserved by the dynamics is given by

$$H(q,p) = \int\limits_{x\in\Omega} \frac{1}{2} p \cdot Bp + W(q)\mathrm{d}x,$$

where $q(t,x) = \partial_x u(t,x) \in L^2(\Omega)$, $p(t,x) = (\rho - \beta\partial_x^2)\dot{u}(t,x) \in H^{-1}(\Omega)$ and $Bp \in H^1(\Omega)$ is the solution of the elliptic equation

$$(\rho - \beta\partial_x^2)v = p, \quad \partial_x v|_{x=0} = 0,\ v|_{x=1} = 0,$$

where $v = Bp$. The symplectic structure is given by the skew-symmetric operator $J = \begin{pmatrix} 0 & \partial_x \\ \partial_x & 0 \end{pmatrix}$. In $u, \dot{u}$-coordinates, the energy takes the form

$$E(u,\dot{u}) = \int\limits_{x\in\Omega} \left(\tfrac{\rho}{2}\dot{u}^2 + W(\partial_x u) + \tfrac{\beta}{2}(\partial_x \dot{u})^2\right)\mathrm{d}x.$$

The expression $K_{\mathrm{mac}} = \frac{\rho}{2}\int_{x\in\Omega} \dot{u}^2\mathrm{d}x$ is called *macroscopic* kinetic energy, $E = \int_{x\in\Omega} W(\partial_x u)\mathrm{d}x$ *elastic* energy, and $K_{\mathrm{mic}} = \frac{\beta}{2}\int_{x\in\Omega}(\partial_x \dot{u})^2\mathrm{d}x$ *microscopic* kinetic energy.

3.1. Qualitative and Quantitative Properties of Typical Solutions

The term $\beta\partial_x^2\ddot{u}$ in (3.1) models the inertia of microscopic structures, e.g., phase boundaries. To give an illustration, we consider a phase boundary which is, at time $t = 0$, at the position $x = 0$ and moves to the right with velocity c. This corresponds to the initial value

$$u_0(x) = \begin{cases} \frac{1}{\kappa}x^2 - x; & x \in [0,\kappa], \\ x - \kappa; & x \in (\kappa, 1], \end{cases}, \qquad v_0(x) = \begin{cases} -\frac{2c}{\kappa}x; & x \in [0,\kappa], \\ -2c; & x \in (\kappa, 1]. \end{cases} \tag{3.2}$$

The variable $\kappa \ll 1$ describes the thickness of the transition layer between the two phases. Using the stored energy function $W(\varepsilon) = \frac{1}{4}(\varepsilon^2 - 1)^2$, we obtain the energy

$$E(u_0, v_0) = (2 - \tfrac{4}{3}\kappa)\rho c^2 + \tfrac{2}{15}\kappa + 2\tfrac{\beta c^2}{\kappa}.$$

This example shows heuristically that the velocity c of the phase boundary has vanishing influence on the elastic and macroscopic kinetic energies if κ is close to 0. Only the microscopic kinetic energy is able to measure the velocity of the phase boundary.

The solution of system (3.1) generated by the above initial condition is by no means a traveling front in the variable $\partial_x u(t,\cdot)$, as can be seen in Figure 2, where the graph of $\partial_x u(t,\cdot)$ is plotted for different values of t. We have used $\sigma(\varepsilon) = E(\varepsilon^3 - \varepsilon)$, the Young modulus $E = 1$ MPa, and the density $\rho = 1\frac{\mathrm{g}}{\mathrm{cm}^3}$ in the numerical simulation. For a precise description of our numerical scheme, error estimates and additional results on the long-time behavior, see Section 6. The solution depicted in Figure 2 has been computed with mirrored boundary conditions, i.e., Dirichlet boundary condition at $x = 1$ and Neumann at $x = 0$. It is obvious that the transition region with thickness κ generates a strongly oscillatory region which is located in the interval $[0,\ 0.2]$. In addition, one can identify a pulse at $x = 0.45$ which is moving at constant velocity to the right.

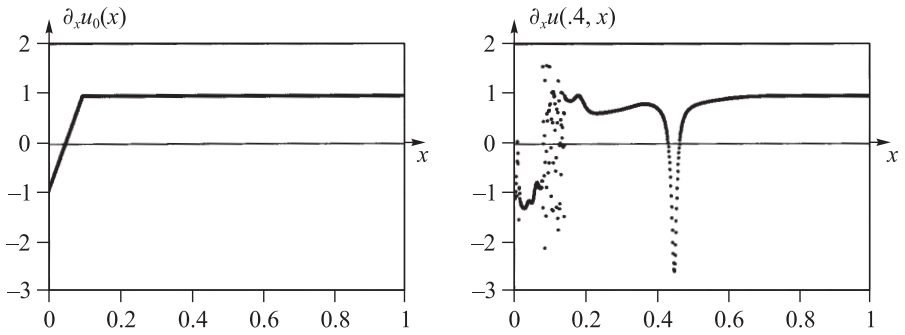

Figure 2. Initial value $\partial_x u_0(\cdot)$, $c = 2$, $\kappa = 0.1$ and a snapshot of the strain $\partial_x u$ at time $t = 0.4$ $(\rho = 1, \beta = 10^{-4})$.

Solitary waves have been found and analyzed for modifications of the Boussinesq equation (2.10) as well as for the improved Boussinesq equation. Formal calculations show that the former equation is completely integrable, while the latter is not, since it does not pass the Painlevé test. This implies that solitary waves may exist but the interaction of two pulses is not elastic, i.e., energy is transferred into high–frequency fluctuations (see [26, 23]). The analysis in [26] shows that the microkinetically regularized wave equation also cannot be expected to be completely integrable. This is confirmed by the results of the numerical simulations.

We find two kinds of solitary waves which we call *nucleation* and *elastic* pulses. The amplitudes of the nucleation pulses are bounded from below, and they traverse the nonmonotone sector of σ completely. The amplitude of the elastic pulses may be arbitrarily small. Elastic pulses have nothing to do with the nonmonotonicity of σ. Rather, they are closely related to the solitary waves which have been analyzed in the Boussinesq equation.

3.2. Nucleation Waves

To discuss traveling waves, we make the usual Ansatz $\partial_x u(t, x) = p(x - ct)$ where $p(\cdot)$ is the initial strain and c is the velocity of the propagation. Substituting p into (3.1), we obtain the ordinary differential equation

$$\rho c^2 p'' = \sigma(p)'' + \beta c^2 p''''.$$

Integrating the above equation twice yields

$$\rho c^2 p = \sigma(p) + \beta c^2 p'' + \lambda + \widetilde{\lambda} x, \tag{3.3}$$

where λ and $\widetilde{\lambda}$ are the constants of integration. We are interested in solutions p satisfying $\lim_{x\to\infty} p(x) = \varepsilon^+$, i.e., nucleations within the phase which is given by the local minimum $\varepsilon = \varepsilon^+$ of W, cf. Figure 1. Using equation (3.3), we find that $\lambda = \rho c^2 \varepsilon^+$ and $\widetilde{\lambda} = 0$ and we end up with the second-order equation

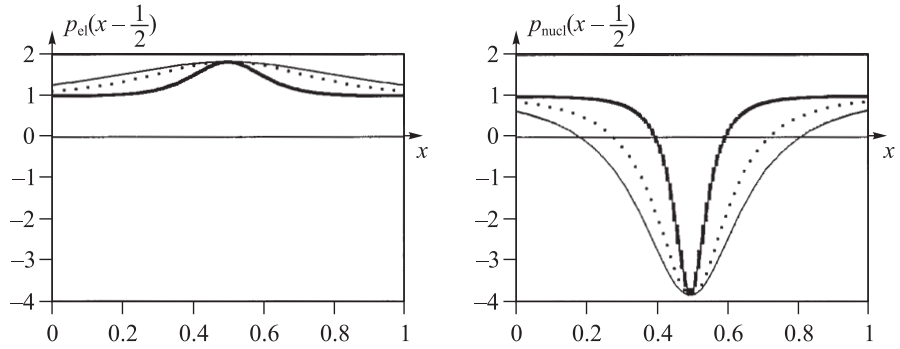

Figure 3. The shape of elastic and nucleation waves for $\rho = 1$, $\mu = 0$, $c = 2$, and $\beta = 0.025$ (–), 0.0125 (· · ·), and 0.0025 (–).

$$\beta c^2 p'' = -\sigma(p) + \rho c^2 p - \rho c^2 \varepsilon^+. \tag{3.4}$$

The solutions of (3.4) move along the equipotential lines

$$\frac{1}{2}\beta c^2 (p')^2 + W(p) - \frac{1}{2}\rho c^2 p^2 + \rho c^2 \varepsilon^+ p = \text{const.}$$

To find a homoclinic orbit attached to the point $y^\infty = (\varepsilon^+, 0) \in \mathbb{R}^2$, the point ε^+ has to be a local maximum of the function $(\varepsilon \mapsto W(\varepsilon) - \rho c^2 \varepsilon(\frac{1}{2}\varepsilon - \varepsilon^+))$, hence $\rho c^2 \geq \sigma'(\varepsilon^+)$. The amplitude A of the pulse is $|\varepsilon^+ - \gamma|$, where γ is the smallest and greatest, respectively, zero of

$$\varepsilon \mapsto \frac{\beta c^2}{2}(\varepsilon')^2 + W(\varepsilon) - \frac{1}{2}\rho c^2 \varepsilon^2 + \rho c^2 \varepsilon^+ \varepsilon - W(\varepsilon^+) - \frac{1}{2}\rho c^2 (\varepsilon^+)^2. \tag{3.5}$$

For the choice $W(\varepsilon) = \frac{1}{4}(\varepsilon^2 - 1)^2 + \mu(\varepsilon - \frac{1}{3}\varepsilon^3)$, which has been used in the numerical simulations, the shape of the pulse can be computed explicitly:

$$p(x) = 1 + \frac{\rho c^2 - 2(1-\mu)}{1 - \frac{\mu}{3} \pm \sqrt{\frac{1}{2}\rho c^2 + \frac{1}{9}\mu(\mu+3)}\cosh\left(\sqrt{\frac{\rho c^2 - 2(1-\mu)}{\beta c^2}}x\right)}.$$

The role of μ will be explained in the following section. Thus, we have obtained two families of pulse solutions (p_{el} and p_{nucl}) moving at velocity c. If $\mu = 0$, one finds the simple velocity-amplitude relation $A(c) = \max_{x\in\mathbb{R}} |\varepsilon^+ - p(x)| = c\sqrt{2\rho} \pm 2$.

For $\rho = 1, c = \sqrt{2}, \mu = 0$, the amplitude $A = 4$ is approximated well by the numerically computed pulse. Note that in the case $\rho = 0$, pulse solutions satisfying $\lim_{|x|\to\infty} p(x) = \varepsilon^+$ do not exist. Of course, these results also hold true with minor modifications, if the stored elastic energy W is given by a more general function than a polynomial of fourth order.

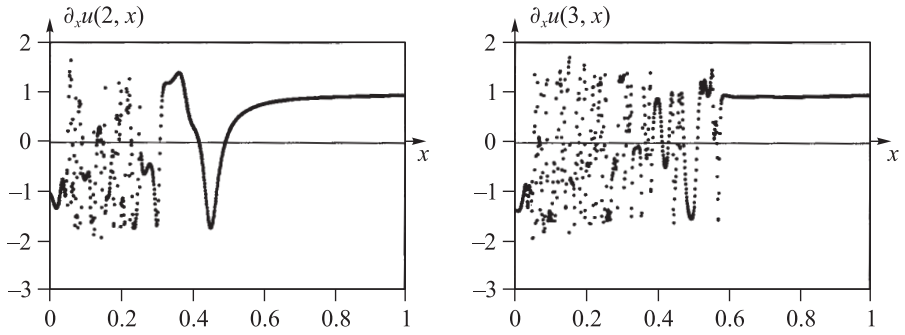

Figure 4. Two snapshots at time $t = 2$ and $t = 3$ show, how a propagating phase-transformation region gets stuck at $x_{\text{term}} = 0.6$ ($\rho = 1$, $\beta = 10^{-2}$, $\mu = 0.5$, $c = 0.2$, $\kappa = 0.1$).

3.3. Propagation of a Phase Transformation Front

To discuss the simulation results concerning the considerations in the introduction, we would like to study the propagation of a phase transformation front. From the preceding discussion of the pulse solutions, it is clear that front solutions cannot exist. Frontlike solutions require that the energy $W(\varepsilon) - \frac{1}{2}\rho c^2\varepsilon^2 + \lambda\varepsilon$ (cf. (3.3)) has two local maxima of equal height at the positions $\varepsilon = \varepsilon^-$ and $\varepsilon = \varepsilon^+$, but this is only possible in degenerate cases which we will not consider in the present work.

The model is intended to describe the dynamics of phase transformations when no dissipation is present. Since the solutions cannot dissipate kinetic energy, the fluctuations due to the phase transformation remain after the transformation region has propagated. Therefore, we expect to observe wild oscillations in the wake of the nucleation pulse. These oscillations should be interpreted as heat since they do not give a contribution to the kinetic energy but only to the microkinetic energy.

We consider a scenario where phase 2 is slightly destabilized, i.e., the boundary force Σ is below the Maxwell-line. It is unpleasant that the local minima of the Gibbs' energy $W(\varepsilon) - \Sigma \cdot \varepsilon$ are only given implicitly – this makes the algebraic manipulations intricate. Therefore, we model the effect of $\Sigma \neq 0$ by taking $\sigma(\varepsilon) = \varepsilon^3 - \varepsilon + \mu \cdot (1 - \varepsilon^2)$ where $\mu \in \mathbb{R}$ is a control parameter, which allows us to destabilize ($\mu > 0$) or to stabilize ($\mu < 0$) phase 2. For $|\mu| \ll 1$, we obtain the relation

$$\mu \sim -\frac{3}{2}\Sigma.$$

The simulation of the solution defined by the initial datum (3.2) shows exactly the expected behavior (see Fig. 4). One can observe a phase transformation front characterized by the tip of the pulse at $x = 0.45$ moving from left to right through the material, leaving a wake of oscillations behind. It is interesting that the phase transformation front comes to a stop when the gained energy is transformed too quickly into microscopic fluctuations. This obstructs the activation of the stable phase and the phase transformation may terminate (see Fig. 4). This astounding effect demonstrates that the study of the qualitative dynamic behavior

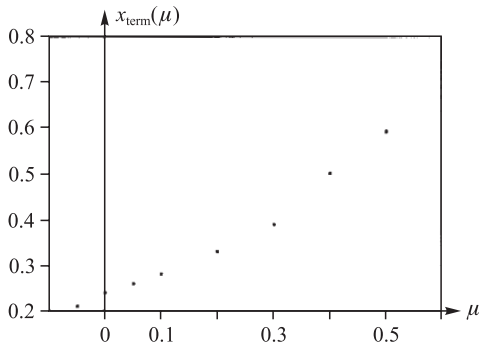

Figure 5. Position of the stuck PT-front for different values of μ.

requires a good understanding of the high-frequency oscillations in space. If the sign of μ is reversed, phase 2 is stabilized and the phase transformation does not even start, i.e., hysteresis is observed. It is highly remarkable that allowance for microkinetic energy results in this phenomenon. In macroscopic models, it is interpreted in terms of a dissipative threshold which the driving force has to overcome to ensure that the phase transformation proceeds (see, e.g., [27, 28]). Moreover, in the numerical simulations, this threshold depends on the volume fraction of transformed phase, which corresponds to the macroscopic description of known experimental results [29, 28]. In Figure 5, the position x_{term}, where the phase transformations stopped, is plotted over different values of μ.

In the numerical simulations, it can be seen that the right-hand boundary influences the dynamics only in a very weak fashion (see Fig. 2). Simple symmetry considerations show that every solution of the microkinetic system can be extended to the enlarged system where $\Omega = (-1, 1)$ and Neumann boundary conditions $\sigma(\varepsilon) + \beta\ddot{\varepsilon} = 0$ are imposed on $x \in \{-1, 1\}$. In more general cases, the Dirichlet boundary condition at $x = 0$ prevents at least an energy exchange between $x > 0$ and $x < 0$. But an outflow of the energy from the transformation region to the left would only increase the dissipative threshold. Therefore, the Dirichlet boundary condition at $x = 0$ has the tendency to decrease the threshold values.

4. THE PROPAGATION OF OSCILLATIONS

The Hadamard instability which is present in equation (1.2) if $\beta = 0$ is not completely removed by the regularization term $\beta\partial_x^2\ddot{u}$. The onset of the fluctuations is delayed: we expect that after time T, the oscillations will occur on a length scale $h = \sqrt{\beta}/T$. Their presence makes a rigorous discussion of the qualitative dynamical behavior very difficult.

Our approach is to study the oscillations which are brought into the system via oscillatory initial states. We do not let β tend to 0; instead, we consider for fixed $\beta > 0$ a sequence of oscillatory initial states and ask: "How do the oscillations propagate as the time increases?" It turns out that they remain stationary in Ω, but the stochastic properties change in a well-defined fashion. To give a motivation, one could think of taking, for $\beta \ll 1$, the solution at

time $t = 1$ (which should look very similar to the simulation result depicted in Fig. 2) as a new initial value.

In the derivation of the constitutive law (2.9), we have assumed that local stresses and strains $\tilde{\sigma}$ and $\tilde{\varepsilon}$ can be replaced by their homogenized counterparts σ_m and ε_m. Thus, the constitutive law (2.9) loses its validity if oscillations occur which have a wavelength shorter than $\sqrt{\beta}$, the size of a characteristic volume. On the other hand, there are only few systems known which support oscillatory solutions. We are not aware of any model where the dynamic creation of microstructure can be studied rigorously. We will ignore the modeling restriction and concentrate on the discussion of oscillatory solutions to the partial differential equation (3.1).

The mathematical analysis of oscillatory solutions consists of several steps. First an integro-differential equation is derived, which allows a clearer view of the structure of the equation. Then we define Young measures and oscillatory solutions in a mathematically rigorous way. The propagation of oscillations is characterized by the extended system (4.2) (see Theorem 4.2). In Section 5, the stationary solutions of the extended system are characterized and discussed. If $\rho = 0$, the long-time behavior or the microkinetic system can be understood completely. Almost every solution generates a nontrivial stationary Young measure as time tends to infinity. The deformation $u(t)$ becomes stationary, but the long-time limit is not an equilibrium solution of (1.2) (Theorem 5.3).

To simplify the analysis for system (3.1), we transform it into an integro-differential equation which does not contain spatial derivatives. The new variables are given by $(\varepsilon, \eta) = \mathcal{T}(u, \dot{u}) = (\partial_x u, \partial_x \dot{u})$. By differentiating equation 3.1 once with respect to x, one obtains

$$(\rho - \beta\partial_x^2)\ddot{\varepsilon} = \partial_x^2 \sigma(\varepsilon).$$

Using the operator $\mathcal{B}$ which has been defined in Section 2, we find that

$$\begin{aligned}
\ddot{\varepsilon} - \ddot{\varepsilon}|_{x=1} &= \rho\mathcal{B}\left(\partial_x^2 \frac{1}{\rho}\sigma(\varepsilon) - \ddot{\varepsilon}|_{x=1}\right) \\
&= -\frac{1}{\beta}\rho\mathcal{B}\left[\left(\rho - \beta\partial_x^2\right)\frac{1}{\rho}(\sigma(\varepsilon) - \sigma(\varepsilon|_{x=1}))\right] \\
&+ \frac{1}{\beta}\rho\mathcal{B}\left[\underbrace{-\sigma(\varepsilon|_{x=1}) - \beta\ddot{\varepsilon}|_{x=1}}_{=0} + \sigma(\varepsilon)\right] \\
&= -\frac{1}{\beta}(\sigma(\varepsilon) - \sigma(\varepsilon|_{x=1})) + \frac{1}{\beta}\rho\mathcal{B}\sigma(\varepsilon) \Rightarrow \ddot{\varepsilon} = -\frac{1}{\beta}(\sigma(\varepsilon) - \rho\mathcal{B}\sigma(\varepsilon)).
\end{aligned}$$

Thus, (ε, η) satisfies the following integro-differential equation

$$\dot{\varepsilon} = \eta, \qquad \varepsilon|_{t=0} = \varepsilon_0 \in L^2(\Omega), \tag{4.1a}$$

$$\dot{\eta} = -\tfrac{1}{\beta}(\sigma(\varepsilon) - k), \qquad \eta|_{t=0} = \eta_0 \in L^2(\Omega), \tag{4.1b}$$

$$k = \rho\mathcal{B}\sigma(\varepsilon), \tag{4.1c}$$

which defines for us a dynamics in $L^2(\Omega, \mathbb{R}^2)$. The evolution preserves the regularity of the solutions, i.e., if $(\varepsilon_0, \eta_0) \in C^1(\Omega, \mathbb{R}^2)$, then $(\varepsilon, \eta)(t) \in C^1(\Omega, \mathbb{R}^2)$ for all $t \geq 0$. The most

important property of this system is that the equations for ε and η are hyperbolic with wave speed 0, and thus the solutions cannot develop shocks. This transport equation allows the system to carry solutions oscillating rapidly in ε and η. Since the spatial coupling via $\rho\mathcal{B}$ is compact, k cannot fluctuate in space.

4.1. Definition of Young Measures and Oscillatory Solutions

A relevant tool for the study of oscillations are Young measures (or parameterized measures) which have gained in importance during the last 20 years. A Young measure $\Psi \in \mathrm{Y}(\Omega, \mathbb{R}^d)$, $d \in \mathbb{N}$, is a mapping from Ω into the set of probability measures on $\mathbb{R}^d$, which is denoted by $PM(\mathbb{R}^d)$. For each $x \in \Omega$, the probability density $\Psi(x)(\cdot)$ measures the probability that the strain and the strain velocity $(\partial_x u^{(n)}, \partial_x \dot{u}^{(n)})$ take the value (ε, η).

In the context of oscillations, Young measures are conceived as a family of one-point distributions which are usually generated by a sequence of rapidly oscillating functions. To clarify the term "generated," we have to become a little bit more technical and introduce notions from probability theory. Let $f^{(n)} : \Omega \to \mathbb{R}$ be a bounded sequence of functions. For a given point $x_0 \in \Omega$, we choose a positive number r, a positive integer n, and a step length h. We intend to consider the limits $h \to 0, n \to \infty$, and $r \to 0$ in this order. The triple (r, n, h) defines a finite sample consisting of the values $f^{(n)}(x_0 + hk), k \in \{\eta \in \mathbb{Z} | x_0 + \eta h \in [x_0 - r, x_0 + r]\}$. Now we let h tend to 0. This generates a unique family of probability measures $\widetilde{\nu}(x_0, r, n, \cdot) \in PM(\mathbb{R}^d)$ which is parameterized over $(x_0, r, n) \in \Omega \times \mathbb{R}^+ \times \mathbb{N}$. If for almost every $x_0 \in \Omega$ the limit $\nu(x_0) = \lim_{r\to 0} \lim_{n\to\infty} \widetilde{\nu}(x_0, r, n)$ exists (in the probability theoretic vague sense), then we say that $f^{(n)}$ generates the Young measure $\nu : \Omega \to PM(\mathbb{R}^d) : x_0 \mapsto \nu(x_0)$.

An alternative characterization, which is more suitable in the context of partial differential equations, is given by the duality of probability measures and continuous functions. A sequence $f^{(n)}$ generates a Young measure Ψ if and only if for every continuous function $g : \mathbb{R}^d \to \mathbb{R}$

$$\lim_{n\to\infty} g(f^{(n)}(x)) \rightharpoonup \langle \Psi(x), g \rangle_{y\in\mathbb{R}^d} \quad \text{weakly in } L^2(\Omega).$$

By "$\langle \cdot, \cdot \rangle$," the duality between probability measures and continuous functions is denoted. To obtain a clear distinction between the variables, the integration variable is used as an index, i.e.,

$$\langle \Psi(x), g \rangle_{y\in\mathbb{R}^d} = \int_{y\in\mathbb{R}^d} g(y) \cdot \Psi(x, y) \mathrm{d}y$$

if the probability measure $\Psi(x)$ has a density $\Psi(x, y)$. By slight abuse of notation, we will adhere to this function notation even if the measure is singular. It is our aim to emphasize the geometric viewpoint by this notation.

We say that the sequence of solutions $u^{(n)}$ defines an oscillatory solution if the initial values $(\partial_x u_0^{(n)}, \partial_x v_0^{(n)})$ generate a nontrivial Young measure Ψ_0.

4.2. Effective Evolution Equations

Spatial oscillations (microstructure) are not damped away by the dynamics of the microkinetic model. A possible characterization of the time evolution of oscillations is given by the following problem:

> Given a sequence of initial states to the microkinetic system $(u_0^{(n)}, v_0^{(n)})$ so that $(\partial_x u_0^{(n)}, \partial_x v_0^{(n)})$ generates a unique Young measure Ψ_0 as $n \to \infty$, does $y^{(n)}(t,x) = (\partial_x u^{(n)}, \partial_x \dot{u}^{(n)})(t,x)$ generate also for $t > 0$ a unique time-dependent Young measure $\Psi(t)$?

It can be shown that the answer is yes: the time-dependent Young measure $\Psi(t,x,y)$ is a distributional solution of the transport equation

$$\partial_t \Psi(t,x,y) + \nabla_y \cdot \{\Psi(t,x,y) \cdot (y_2, -\frac{1}{\beta}(\sigma(y_1) - k(t,x)))^t\} = 0, \ \Psi|_{t=0} = \Psi_0, \quad (4.2a)$$

$$(\rho - \beta\partial_x^2)k(t,x) = \rho\langle \Psi(t,x,y), \sigma(y_1)\rangle_{y\in\mathbb{R}^2}, \ \partial_x k|_{x=0} = 0, \ k|_{x=1} = 0. \quad (4.2b)$$

The transport term is exactly the right-hand side of system (4.1). Equation (4.2a) has to be read in the weak sense, i.e., for every test function $g \in C^1(\mathbb{R}^2)$,

$$\frac{\mathrm{d}}{\mathrm{d}t}\langle \Psi, g\rangle - \langle \Psi(t,x,y), \nabla g(y) \cdot (y_2, -\frac{1}{\beta}(\sigma(y_1) - k(t,x)))^t\rangle_{y\in\mathbb{R}^2} = 0 \quad (4.3)$$

for every $x \in \Omega$. System (4.2) is an extension of (3.1), i.e., every solution of (3.1) is a special solution of (4.3). We formulate this fundamental assertion in

Proposition 4.1. *Let $u(t,x)$ be a solution of (3.1) and $\varepsilon = \partial_x u$, $\eta = \partial_x \dot{u}$. Then the Young measure*

$$\Psi(t,x) = \delta_{(\varepsilon,\eta)(t,x)},$$

where δ_y is the Dirac distribution with mass at $y \in \mathbb{R}^2$, which is a distributional solution of (4.2).

Proof. Since the equivalence of (3.1) and (4.1) has already been established, we set $y(t,x) = \mathcal{T}(u(t,x), \dot{u}(t,x))$. By inserting $\delta_{y(t,x)}$ into (4.3), we obtain

$$\frac{\mathrm{d}}{\mathrm{d}t} g(y(t)) - \nabla g(y(t)) \cdot (y_2, -\frac{1}{\beta}(\sigma(y_1) - k(t,x)))^t = 0$$

by (4.1). □

It can be shown under reasonable assumptions that the solutions of (4.2) are unique and exist globally in time. The central assertion which justifies (4.2) as an effective equation for oscillatory solutions is the following continuity result. If the oscillations of the initial state can be captured with a Young measure Ψ_0, it suffices to take Ψ_0 as an initial value for (4.2). The unique solution at time t is a Young measure which describes the oscillations at time t.

Theorem 4.2. *Let* $(\partial_x u_0^{(n)}, \partial_x v_0^{(n)}) \in L^2(\Omega, \mathbb{R}^2)$ *generate the Young measure* $\Psi_0 \in \mathrm{Y}(\Omega, \mathbb{R}^2)$ *and* $u^{(n)}(t)$ *be a sequence of solutions to the microkinetically regularized wave equation (3.1), so that* $(\partial_x u^{(n)}, \partial_x \dot{u}^{(n)})(t=0) = (\partial_x u_0^{(n)}, \partial_x v_0^{(n)})$. *Then* $(\partial_x u^{(n)}, \partial_x \dot{u}^{(n)})(t)$ *generates a Young measure* $\Psi(t)$, *which is the unique solution of (4.2) satisfying the initial condition* $\Psi(0) = \Psi_0$.

Proof. For a proof, see [30, 31]. □

It is not at all clear that Young measures are always the right objects to capture oscillatory behavior since they ignore spatial correlations. In higher dimensional settings, it can be shown that mathematically more elaborate objects than one-point statistics are needed. However, for this prototypical one-dimensional equation, they suffice. For a general discussion on the relation between Young-measure solutions and classical solutions of generalizations of system (4.1), see [32].

We summarize the results of this section. Replacing the original coordinates displacement-velocity $(u, \dot{u})$ by the new coordinates strain-strain rate (ε, η), it was possible to transform system (3.1) into the equivalent, mathematically more accessible system (4.1). This system supports oscillating solutions, and one can show that the dynamics of oscillatory solution can be described with time-dependent Young measures which are unique solutions of (4.2). Thus, the latter equation is a homogenized version of (4.1): it describes the macroscopic behavior of the microscopically fluctuating strain.

5. LONG-TIME BEHAVIOR

The discussion of the dynamics of the microkinetically regularized wave equation (1.2) shows that the stationary solutions of (4.2) are central for the understanding of the qualitative behavior. They represent a kind of oscillatory ground state, which is to a large extent independent from the macroscopic dynamics.

In the numerical simulation results in Section 3, one can see that the phase transformation induces strong oscillations in the solutions. The macroscopic dynamics of these oscillatory solutions is very slow, suggesting the supposition that they approximate stationary Young measures. This supposition is partly supported by the results of Section 5.2. In the case $\rho = 0$, the spatial averages of generic solutions relax, even stronger $(\partial_x u, \partial_x \dot{u})(t)$ generates a nontrivial stationary Young measure as time tends to infinity. This means the macroscopic kinetic energy is transformed into microscopic kinetic energy. For nonzero ρ, relaxation toward an oscillatory state in the sense of Young measures can be confirmed neither analytically nor numerically. The solutions still develop arbitrarily fine oscillations, but a certain amount of macroscopic dynamics remains in the simulations.

Since the microkinetic system (3.1) is Hamiltonian, it might be surprising, at first glance, that generic solutions may converge to an equilibrium for $t \to \infty$. This is only possible by developing fine oscillations so that the macroscopically visible kinetic energy vanishes into microscopic fluctuations. If not only the linear averages but also all n–point distributions would converge, one could speak of thermalization, the typical behavior of solids in the absence of exciting forces. The fundamental laws of physics are reversible. So the introduction of additional quantities like temperature, which are necessary to describe

irreversible processes, only gives a model–like, statistical description of this behavior. Of course the convergence of the displacement $u(t)$ says nothing about the correlations, and, in fact, in our model one cannot expect that two–point functions like $\frac{1}{|B(0,r)|}\int_{B(0,r)} \varepsilon(t,x_1+y)\cdot \varepsilon(t,x_2+y)\,\mathrm{d}y$ converge.

5.1. Generalized Stationary States

To clarify the role of system (4.2), we demonstrate that the system is a nontrivial extension of (4.1). This is done by comparing the set of equilibrium points $\mathcal{C}$ of (3.1) with the equilibria $\mathcal{Y}$ of (4.2). It turns out that $\mathcal{Y}$ is much larger than $\mathcal{C}$: the latter set is not even dense in the former. The stationary points of (3.1) are characterized by the equation $\partial_x\sigma(\partial_x u)=0$. Using the Neumann boundary condition, this equation can be integrated once and one obtains $\sigma(\partial_x u)=0$. We denote the three zeros of σ by z_i where $\varepsilon^- < z_0 < \varepsilon^+$. The set of equilibrium points can be characterized as follows: for every stationary solution u^* of (3.1), there exists a partition $(\Omega_1,\Omega_0,\Omega_2)$ of Ω so that $\partial_x u^*(x)=\sum_{i=0}^2 \chi_{\Omega_i}(x) z_i$ almost everywhere.

The equilibrium points of the extended system (4.2) are defined by the equation

$$\begin{aligned} \langle \Psi(x,y), \nabla g(y)\cdot(y_2, -\frac{1}{\beta}(\sigma(y_1)-k(x)))^t\rangle_{y\in\mathbb{R}^2} &= 0, &(5.1)\\ (\rho-\beta\partial_x^2)k &= \rho\langle \Psi(x,y),\sigma(y_1)\rangle_{y\in\mathbb{R}^2} &(5.2)\end{aligned}$$

for every test function $g\in C^1(\mathbb{R}^2)$. By choosing $g(y)=y_2$, we obtain the relation

$$\langle \Psi(x,y), -\frac{1}{\beta}(\sigma(y_1)-k(x))\rangle_{y\in\mathbb{R}^2}=0$$

for every $x\in\Omega$. Hence (5.2) implies $k=0$. Thus, it suffices to analyze the equation

$$\begin{aligned} \nabla_y\cdot\{\Psi\cdot(\beta y_2,-\sigma(y_1))^t\} &= 0\\ \Leftrightarrow\ \nabla\Psi(x,y)\cdot J\cdot\nabla H(y) &= 0,\quad J=\begin{pmatrix}0&1\\-1&0\end{pmatrix}, &(5.3)\end{aligned}$$

where $H(y)=\frac{\beta}{2}y_2^2+W(y_1)$. Equation (5.3) expresses the fact that, for fixed $x\in\Omega$, the function $\Psi(x,y)$ is constant on the connected components of the equipotential lines of H. For the convenience of the reader, we give a short proof of this well-known fact.

Lemma 5.1. Let $\Psi, H\in C^1(\mathbb{R}^2,\mathbb{R})$ and

$$\partial_{y_1}\Psi\cdot\partial_{y_2}H=\partial_{y_2}\Psi\cdot\partial_{y_1}H \tag{5.4}$$

for every $y\in\mathbb{R}^2$. Let in addition $y^1,y^2\in\mathbb{R}^2$ and $\varphi\in C^1([0,1],\mathbb{R}^2)$ satisfying $\varphi(0)=y^{(1)}$, $\varphi(1)=y^{(2)}$, and $\frac{\mathrm{d}}{\mathrm{d}t}H(\varphi(t))=0$ for every $t\in[0,1]$. Then $\Psi(y^{(1)})=\Psi(y^{(2)})$ holds.

Proof. We have that $\Psi(y_2)-\Psi(y_1)=\int_0^1\nabla\Psi(y(t))\cdot\dot{y}(t)\mathrm{d}t=0$ because of (5.4) and since $\frac{\mathrm{d}}{\mathrm{d}t}H(y(t))=\nabla H(y(t))\cdot\dot{y}$. □

For double well potentials like $W(\varepsilon) = \frac{1}{4}(\varepsilon^2 - 1)^2$, we have to split the phase space $\mathbb{R}^2$ into three domains to represent arbitrary phase distributions:

$$\begin{aligned} P_1 &= \{y \in \mathbb{R}^2 | H(y) < W(z_0) \text{ and } y_1 < z_0\}, \\ P_2 &= \{y \in \mathbb{R}^2 | H(y) < W(z_0) \text{ and } y_1 > z_0\}, \\ P_0 &= \mathbb{R}^2 \setminus (P_1 \cup P_2). \end{aligned} \tag{5.5}$$

The sets P_1 and P_2 correspond approximately to the two stable phases ε^- and ε^+. By Lemma 5.1, every stationary solution $\Psi^*(x,y)$ of (4.2) can be expressed using three functions:

Theorem 5.2. *Let Ψ be a stationary solution of (4.2) which has a density function $\Psi^* : \Omega \times \mathbb{R}^2 \to \mathbb{R}_{\geq}$. Then there exist three functions $\alpha_i : \Omega \times \mathbb{R}^+ \to \mathbb{R}^+$, $i = 0, 1, 2$ so that*

$$\Psi^*(x,y) = \sum_{i=0}^{2} \chi_{P_i}(x) \cdot \alpha_i(x, H(y)),$$

where P_0, P_1, P_2 is the partition of $\mathbb{R}^2$ defined by (5.5).

The converse of the theorem also holds true if α_i satisfy normality constraints like $\langle \Psi^*(x,y), 1 \rangle_{y \in \mathbb{R}^2} = 1$ for every $x \in \Omega$. By taking suitable sequences $(\alpha_i^k)_{k \in \mathbb{N}}$, we also obtain singular equilibria. The notation of the singular equilibrium Young measures requires the use of geometric measure theory, so we have decided not to characterize the full set of stationary solutions in this work.

Very similar results concerning stationary Young measures for a two-dimensional magneto fluid have been obtained in [17, 18]. There, the most probable stationary states are determined by the maximum of an entropy functional. In our case, the importance of the stationary Young measures is not clear if $\rho > 0$ (cf. the results of the long-time integrations in Section 6).

The striking difference between the stationary solutions of (3.1) and stationary Young measures is that the latter may have nonvanishing velocity components, while classical equilibria are restricted to the line $\eta = 0$. Since the velocity distribution of stationary Young measures is symmetric with respect to $\eta = 0$, the average velocity $\langle \Psi(x,y), y_2 \rangle_{y \in \mathbb{R}^2}$ vanishes for every $x \in \Omega$. One should also note that the displacement $u^*(x)$ associated with a stationary Young measure $\Psi^*(x)$ via

$$u^*(x) = \int_0^x \langle \Psi^*(x', y), y_1 \rangle_{y \in \mathbb{R}^2} \, \mathrm{d}x'$$

is not in general a stationary solution of (3.1). This is no contradiction to the fact that Ψ^* is an equilibrium since the microscopic fluctuations are not visible from the macroscopic level. The discussion of the stationary solutions shows that the continuation of equation (3.1) in the space of Young measures reveals many stationary solutions which have been formerly hidden.

5.2. Relaxation toward Oscillatory States

The first attempt to observe the rise of uncorrelated microscopic fluctuations is described in the well-known paper of Fermi, Pasta, and Ulam [19]. The result, which is obtained by numerical integration of several discretized one-dimensional quasilinear wave equations, is truly opposite to the expected behavior. It is found that the motion of the rod is almost periodic, in particular, the solution repeatedly returns, within a fixed accuracy, to the initial configuration.

We say that the spatial averages of a time-dependent strain field $\varepsilon(t)$ relax if for $t \to \infty$ it converges weakly to some time- independent function ε^∞, i.e., $\int_{x\in\Omega} (\varepsilon(t,x) - \varepsilon^\infty(x)) \cdot \phi(x)\mathrm{d}x \to 0$ for every smooth testfunction ϕ. A mechanical interpretation of this notion is the transformation of kinetic energy into heat; only the macroscopic strain ε^∞ remains observable. For $\rho = 0$, system (3.1) exhibits this behavior, almost every solution $u(t,x)$ converges to a stationary function $u^*(x)$ in $L^\infty(\Omega)$ at t to infinity, i.e., (3.1) is a good candidate to study the transformation of macroscopic kinetic energy into heat. But not only $u(t)$ converges but also $(\partial_x u(t,x), \partial_x \dot{u}(t,x))$ generates a unique nontrivial equilibrium Young measure Ψ^* as time goes to infinity. Thus, equation (3.1) is also an example for the dynamic creation of microstructure. The case $\rho = 0$ is an important limit since the equations of motion for $\rho > 0$ emerge from the unperturbed system via a compact perturbation. Thus, one may hope that the essential dynamics can be understood by analyzing the case $\rho = 0$.

The convergence of the solutions if $\rho = 0$ is due to the fact that the system is completely integrable, so it can be analyzed easily using canonical variables.

Theorem 5.3. *Let $\rho = 0$ and $u(t,x)$ be a solution of system (3.1) generated by the initial condition $(u,\dot{u})|_{t=0} = (u_0, v_0)$ and let the genericity assumption $\mathrm{closure}(G) = \Omega$ be fulfilled, where the subset $G \subset \Omega$ is defined as follows:*

$$G = \left\{ x \in \Omega \quad \middle| \quad \frac{\mathrm{d}}{\mathrm{d}x} \int_{\varepsilon\in\mathbb{R}} \Re \left(\frac{\beta}{2}(\partial_x v_0(x))^2 + W(\partial_x u_0(x)) - W(\varepsilon) \right)^{-\frac{1}{2}} \mathrm{d}\varepsilon \neq 0 \right\}.$$

Then there exists a unique nontrivial stationary Young measure $\Psi^* \in \mathrm{Y}(\Omega, \mathbb{R}^2)$ so that $(\partial_x u(t,x), \partial_x \dot{u}(t,x))$ generates Ψ^* for $t \to \infty$.

Using this abstract result, one can easily deduce the following theorem which describes the long–time behavior of solutions more graphically.

Theorem 5.4. *Let $u(t,x)$ be a solution of (3.1) and let the assumptions of Theorem (5.3) be satisfied. Then there exists a function $u^*(x)$ so that $\lim_{t\to\infty} \|u(t,x) - u^*(x)\|_{L^\infty(\Omega)} + \lim_{t\to\infty} \|\dot{u}(t,x)\|_{L^\infty(\Omega)} = 0$. If in addition $G = \Omega$, then there is a constant $C > 0$ so that $\|u(t,x) - u^*(x)\|_{L^\infty(\Omega)} + \|\dot{u}(t,x)\|_{L^\infty(\Omega)} \leq C/\sqrt{t}$.*

For the proofs of both theorems, see [30, 31]. An illustration for the latter theorem can be found in Figure 6 where the solution generated by the initial state $u_0(x) = x^2 - x$, $v_0 = 0$ is plotted for different values of t.

Crucial for this result is the nonmonotonicity of σ. If σ is linear, the set G in Theorem (5.3) is empty since the integral is constantly equal to $2\pi\sqrt{\beta/\sigma'}$. Thus, the relaxation process is strongly related to the underlying phase transformation problem.

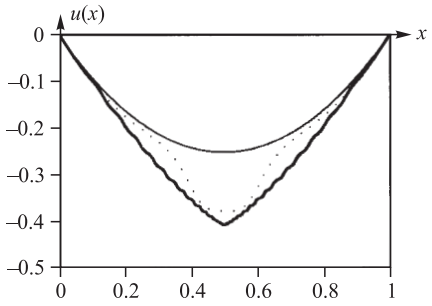

Figure 6. Displacement $u(t)$ for $\rho = 0$, $\beta = 0.01$, $t = 0$ (–), $t = 1$ ($\cdots$), and $t = 10$ (–).

The discussion of the stationary solutions of the microkinetic system reveals that there exist a great variety of Young measure equilibria, which cannot be approximated with classical stationary solutions. The set of the generalized equilibria is very important for the dynamics: it can be shown that it attracts generic solutions in the case $\rho = 0$. The simulation results show that also in the coupled case $\rho > 0$, the solutions stay close to the stationary Young measures.

6. NUMERICAL SCHEME AND SIMULATION RESULTS

Since there are no rigorous results concerning the long-time behavior if $\rho > 0$ is considered, we present some numerical results which should illuminate the qualitative behavior in the coupled case. The results indicate that the asymptotics for $\rho > 0$ differ from the uncoupled case. Before we comment on the individual long–time integrations, we explain the notion of convergence of the numerical scheme. For simplicity, we set $\beta = 1$.

A Young-measure solution is approximated by aggregated Young measures:

$$\mathrm{Y}^{h,N}(\Omega,\mathbb{R}^2) = \left\{ \Psi \in \mathrm{Y}(\Omega,\mathbb{R}^2) \,\middle|\, \Psi(x) = \tfrac{1}{N} \sum_{k=0}^{\frac{1}{h}-1} \sum_{i=1}^{N} \chi_{[hk,h(k+1))}(x) \delta_{y^{ik}} \text{ where } y \in \mathbb{R}^{N\times\frac{1}{h}\times 2} \right\}.$$

Aggregated Young measures $\Psi^{h,N} \in \mathrm{Y}^{h,N}(\Omega,\mathbb{R}^2)$ are constant on intervals of length h. For $x \in (hk, h(k+1))$, the probability measure $\Psi^{h,N}(x)$ is a convex combination of N Dirac masses located at $\{y^{ik}, i = 1 \ldots N\}$. We remark that there are various possibilities for approximating nontrivial Young measures by simpler objects. For a discussion of some methods, see Roubicek's book [33], Section 4.

To obtain useful estimates, we introduce a metric which has the property that $\cup_{M,N=1}^{\infty} \mathrm{Y}^{\frac{1}{M},N}(\Omega,\mathbb{R}^2)$ is dense in $\mathrm{Y}(\Omega,\mathbb{R}^2)$. We define

$$d_2(\Psi_1,\Psi_2) = \left\| \sup_{\|\nabla g\|_{L^\infty(\mathbb{R}^2)} \le 1} \langle \Psi_1(x) - \Psi_2(x), g \rangle \right\|_{L^2_x(\Omega)},$$

where the subscript x denotes the integration variable of the L^2-norm. The metric $d_2(\cdot,\cdot)$ is an extension of the Wasserstein distance which meterizes vague convergence in the space of probability measures with first moment, see, e.g., [34]. Of course, for given $\Psi \in \mathrm{Y}(\Omega,\mathbb{R}^2)$ there is no a priori estimate for $\inf_{\Psi^{h,N} \in \mathrm{Y}^{h,N}(\Omega,\mathbb{R}^2)} d_2(\Psi^{h,N},\Psi)$ independent of Ψ which can be used to compute in advance how h and N have to be chosen in order to obtain a prescribed accuracy. The propagation of this initial error can be controlled by using the continuity of the solution with respect to the initial value.

Only if $\rho = 0$ is $\mathrm{Y}^{h,N}$ invariant under the evolution defined by (4.2). For nonvanishing ρ, the right-hand side has to be projected on $\mathrm{Y}^{h,N}$. This motivates the consideration of the modified evolution equation

$$\begin{aligned} \dot{\Psi}^h &= -\nabla_{(\varepsilon,\eta)} \cdot \left\{ \Psi^h \cdot \left(\eta, -\left(\sigma(\varepsilon) - \pi_h \rho \mathcal{B}\left\langle \Psi^h, \sigma \right\rangle\right)\right)^t \right\}, \\ \Psi^h|_{t=0} &= \Psi_0 \in \mathrm{Y}\left(\Omega,\mathbb{R}^2\right). \end{aligned} \tag{6.1}$$

The linear mapping π_h^k is the projection onto the space of piecewise constant functions: $\pi_h^k f(x) = -\frac{1}{h}\int_{x\in[kh,(k+1)h]} f(x')\mathrm{d}x'$ for $x \in [kh,(k+1)h)$. The dynamics defined by (6.1) leaves $\mathrm{Y}^{h,N}$ invariant. For initial values $\Psi_0^{h,N} \in \mathrm{Y}^{h,N}(\Omega,\mathbb{R}^2)$, we obtain

$$\Psi^{h,N}(t,x) = \frac{1}{N}\sum_{k,i} \chi_{[kh,(k+1)h)}\ \delta_{y^{ki}(t)},$$

where the $(\frac{1}{h}\times N\times 2)$-vector $y^{ki}(t)$ solves the ordinary differential equation

$$\dot{y}^{ki} = \begin{pmatrix} y_2^{ki} \\ -\sigma(y_1^{ki}) + \pi_h^k \mathcal{B}\left[\frac{1}{N}\sum_{k,i}\chi_{[kh,(k+1)h)}\ \sigma(y_1^{ki})\right] \end{pmatrix}, \quad y^{ki}(0) = y_0^{ki}. \tag{6.2}$$

This system can be integrated using an arbitrary integration scheme for ordinary differential equations. For the error accumulated due to the modification of the spatial coupling, an exponential bound can be derived.

Theorem 6.1. *Let $\beta = 1$ and $\Psi(t)$ and $\Psi^{h,N}(t)$ solutions of (4.2) and (6.1) satisfying the initial condition $\Psi(0) = \Psi^{h,N}(0) = \Psi_0^{h,N} \in \mathrm{Y}^{h,N}(\Omega,\mathbb{R}^2)$. Then there exist numbers $C_1(\Psi_0)$ and $C_2(\rho, \|\sigma'\|_{L^\infty(\mathbb{R})})$ so that*

$$d_2(\Psi(t), \Psi^{h,N}(t)) \le C_1\sqrt{\rho}h^2 e^{C_2 t}$$

holds.

Proof. See appendix. □

To control the error, when arbitrary initial states are considered, one has to use Gronwall estimates for the Young-measure semiflow. This does not contribute to the understanding of the numerical scheme; therefore, this step is omitted here, see, however, [31].

In the numerical simulations in this work, we used $N = 1$, i.e., only functions, not general Young measures. The reason we proved the convergence for the generalized scheme is that

we are convinced that the numerical results give a good picture of the qualitative dynamics although h and the time increment τ are too large to see the asymptotic regime of the scheme. Theorem 6.1 shows that it is possible to follow solutions which are strongly oscillating. For a proper implementation of these ideas, more sophisticated numerical techniques like adaptive schemes have to be used, but this is beyond the scope of this work.

6.1. Numerical Results

To check the decay of macroscopic kinetic energy, long-time integrations were performed. This might seem dubious since the error grows exponentially in time. At first it seems that the numerically computed solution has nothing to do with the exact solution for large times. The same problem occurs when integration schemes for ordinary differential equations are analyzed; only estimates which behave exponentially in time can be derived. This situation greatly improves if the viewpoint is slightly changed: For integration schemes for ordinary differential equations, it can be shown that the numerically computed solution corresponds to a high precision to a slightly perturbed vector field; more precisely, it can be shown that the error remains exponentially small over a time interval $T = \mathcal{O}(\frac{1}{\triangle t})$ (see, e.g., [35]). Since we are only interested in qualitative properties of the dynamics generated by certain vector fields, this weakened result is satisfactory. It is not our aim to give rigorous estimates for the long-time integrations; we just point out the ideas which are relevant if a rigorous justification of the validity of the results of the long-time integrations is attempted.

As integration method for the system of ordinary differential equations, the implicit midpoint rule with step length $\tau = 0.1$ is used. Equation (6.2) is integrated for different values of ρ over the interval $[0, 400]$, the parameter β being constantly kept to 1. The solutions which are computed in the described fashion conserve the total energy not exactly, but up to a precision of 1% over the whole time interval. For test purposes, we reduced τ to the value 0.01, whereupon the total energy was conserved up to an error of 0.01% and the qualitative results were practically unchanged.

To be able to compare the results for different values of ρ, the initial value is $u_0(x) = \sqrt{2}x + \frac{1}{2}x^2$, $v_0(x) = 0$ in every experiment.

The simulations have been performed with different values of h ($h_1 = 0.005, h_2 = 0.002, h_3 = 0.001, h_4 = 0.0005$). The results of runs using $h = h_3$ and $h = h_4$ differ very little from each other, so it can be expected that the numerical results for $h = h_4$ are in agreement with the exact behavior.

The normalized macroscopic kinetic energy $M(t) = \frac{1}{\rho}K_{\mathrm{mac}}(t) = \frac{1}{2}\int_{x\in\Omega} \dot{u}^2 \mathrm{d}x$ serves as an indicator for the qualitative long-time dynamics. In Figures 7 through 11, the value $M(t)$ is plotted over time in double logarithmic scale. Time t and normalized kinetic energy $M(t)$ are plotted horizontally and vertically, respectively. The first experiment is the uncoupled case $\rho = 0$. One can see clearly that $M(t)$ converges to 0 for $t \to \infty$. The convergence rate of the computed solution is even better than the analytical result: $M(t) \leq C/t$ for some constant $C > 0$. Since $M(t)$ is oscillating strongly within the large integration interval, the graph $\{(t, M(t))|\ t \in [0, 400]\}$ resembles a region more than a line.

In the coupled case ($\rho > 0$), the behavior of the solutions is more complex than in the uncoupled case. On the one hand, in the beginning the solutions develop fine structure, otherwise $M(t)$ would not decay. On the other hand, this process is soon hidden by chaotic

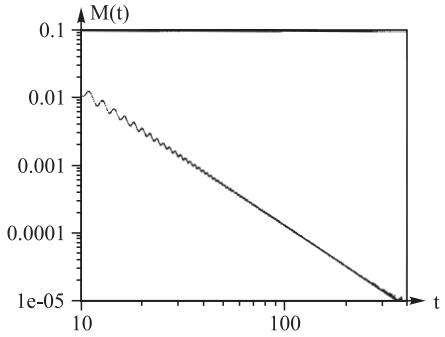

Figure 7. Macroscopic kinetic energy over time, $\rho = 0$, $n = 2000$.

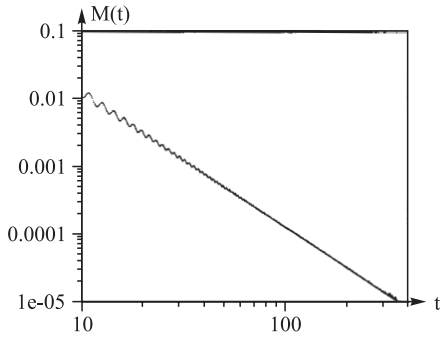

Figure 8. $\rho = 0.02$, $n = 2000$.

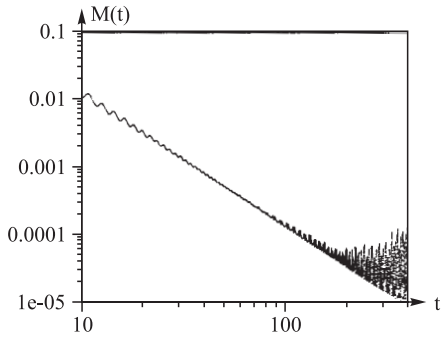

Figure 9. $\rho = 0.05$, $n = 2000$.

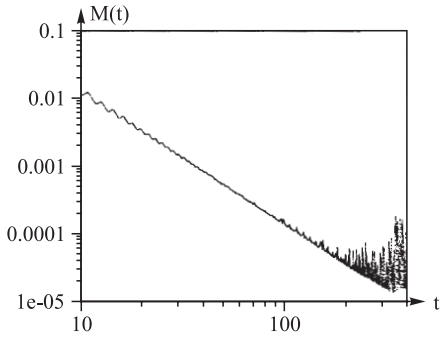

Figure 10. $\rho = 0.1$, $n = 2000$.

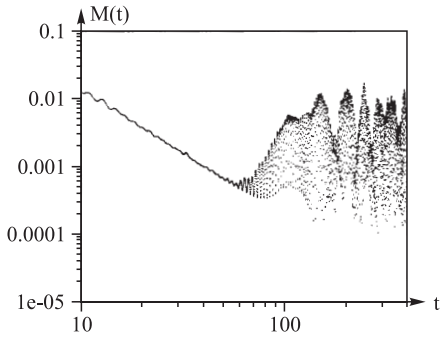

Figure 11. $\rho = 0.2$, $n = 2000$.

oscillations which no longer decay. The nonvanishing of $M(t)$ as $t \to \infty$ is due to the nontrivial coupling. With growing values of ρ, the amplitude of the chaotic oscillations becomes larger. This can be seen in the results for $\rho = 0.02$ (Fig. 8), $\rho = 0.05$ (Fig. 9), $\rho = 0.1$ (Fig. 10), and $\rho = 0.2$ (Fig. 11). These results indicate that the long-time behavior of the solutions in the coupled case cannot be understood by an analysis which is only based on considerations made for the uncoupled case.

7. CONCLUDING REMARKS

In general, high-frequency oscillations due to inertial stresses are not observable at the macro level and represent the continuum mechanical counterpart of thermal fluctuations. Such stress fluctuations can overcome the stress and energy barrier (BCD) in Figure 1 when macroscopic stress-strain curve follows the Maxwell line.

The possible scenario is as follows. After some macroscopic perturbation (e.g., prescribed velocity at the boundary), macroscopic kinetic energy transforms into microscopic kinetic energy, or energy of stress fluctuations. Such energy exists in each specimen before experiment. When, under prescribed growing displacement, macroscopic stress reaches the Maxwell stress and stress fluctuations are sufficient to overcome the barrier (BCD) in Figure 1, then PT will occur at constant stress.

If, for conservative systems, the macroscopic kinetic energy transforms into microscopic kinetic energy, which is not observable macroscopically, then this can be considered as a macroscopic dissipation mechanism. Indeed, the numerical simulations of the microkinetic model presented in this paper exhibit the hysteretic behavior. Such behavior is usually interpreted in macroscopic models in terms of a dissipative threshold which the driving force has to overcome for the phase transformation to proceed. The threshold value depends on the amount of the transformed phase as it is observed in known experiments.

In our model, the transformation of the energetically less favorable phase ε^+ into ε^- is initiated by a nucleation pulse. The macroscopic kinetic energy of the system is transformed into microkinetic energy by the onset of strong oscillations. This process decreases the macroscopic kinetic energy of the system, and the nucleation pulse becomes unstable and collapses finally. To quantify this picture, the notion of Young-measure solutions has been introduced. It has been shown that the extended system, which describes the dynamics of oscillatory solutions, has nontrivial equilibria which can store the microkinetic energy.

We conjecture that the chaotic fluctuations are very close to a unique "most probable" Young-measure equilibrium in the big set of stationary Young measures. The notion of a probable state is meant in the sense of statistical physics, where the Gibbs distributions are identified as maximizers of the entropy.

Most questions concerning the dynamics of the microkinetically regularized wave equation are still open:

It should be possible to obtain a bound C depending on ρ so that the macroscopic kinetic energy is bounded by $C(\rho)$ as time goes to infinity. i.e.,

$$\limsup_{t\to\infty} K_{\mathrm{mac}}(t) \leq C(\rho).$$

What happens if the more physical limit $\rho = 1, \beta \to 0$ is taken? Does the solution u^β converge to solutions of the convexified equation

$$\rho \ddot{u} = \partial_x \sigma^M (\partial_x u),$$

where σ^M is obtained from σ by replacing the nonmonotone part by the Maxwell line? This is only meaningful for smooth solutions. In the case of shocks, the question is more delicate due to the nonuniqueness of weak solutions.

APPENDIX

Proof of Theorem 6.1. We follow the usual procedure to establish the convergence of a numerical scheme: Consistency and stability imply convergence. For the given exact Young measure solutions $t \mapsto \Psi(t,x)$ and $t \mapsto \Psi^{h,N}(t,x)$ of (4.2) and (6.1), we define $\phi(t,x) : \mathbb{R}^2 \to \mathbb{R}^2 : y \mapsto \phi(t,x,y)$ as the family of diffeomorphisms generated by the ordinary differential equation:

$$\dot{\phi}_1(t,x) = \phi_2(t,x), \quad \dot{\phi}_2(t,x) = -\left(\sigma(\phi_1(t,x)) - \rho \mathcal{B} \langle \Psi(t,x,y), \sigma(\phi_1(t,x,y)) \rangle_{y \in \mathbb{R}^2}\right).$$

Correspondingly, the solution flow of the discretized system

$$\dot{q}^h = p^h, \quad \dot{p}^h = -\left(\sigma(q^h) - \pi_h \rho \mathcal{B} \langle \Psi^{h,N}(t,x), \sigma \rangle\right)$$

is denoted by $\phi^h(t,x)$. Note that it follows immediately from equation (4.3) that Ψ and $\Psi^{h,N}$ satisfy

$$\langle \Psi(t), g \rangle_{y \in \mathbb{R}^2} = \langle \Psi_0, g \circ \phi(t,x) \rangle_{y \in \mathbb{R}^2},$$

and

$$\langle \Psi^{h,N}(t), g \rangle_{y \in \mathbb{R}^2} = \langle \Psi_0^{h,N}, g \circ \phi^h(t,x) \rangle_{y \in \mathbb{R}^2},$$

for every test function $g \in C(\mathbb{R}^2)$.

Consistency of $\rho\mathcal{B}$ with $\pi_h \rho \mathcal{B}$

We establish the existence of a constant $C > 0$ so that

$$\|(Id - \pi_h)\rho\mathcal{B}\|_{\mathrm{Lin}(L^2(\Omega), L^2(\Omega))} \leq Ch^2]$$

holds. This results mainly from the smoothing property of $\rho\mathcal{B}$. We set $\omega_k = [hk, h(k+1)) \subset \mathbb{R}$. First, $\|\pi_h u - u\|_{L^2(\Omega)}$ is estimated by $\|\partial_x u\|_{L^2(\Omega)}$. Using the intermediate value theorem for every $k \in \{0, \ldots 1/h - 1\}$, one obtains the existence of $\xi_k \in \omega_k$ so that $\fint_{x \in \omega_k} u(x)x = u(\xi_k)$ holds. Hence

$$\left| \fint_{x' \in \omega_k} u(x')x' - u(x) \right| = |u(\xi_k) - u(x)| \leq \int_{\xi_k}^{x} |u'(s)| \, \mathrm{d}s \leq \sqrt{|x - \xi_k|} \left(\int_{\xi_k}^{x} |u'(s)|^2 \, \mathrm{d}s \right)^{\frac{1}{2}}.$$

Using this estimate, we obtain

$$\begin{aligned}
\left(\int_\Omega |\pi_h u(x) - u(x)|^2 \, \mathrm{d}x \right)^{\frac{1}{2}} &= \left(\sum_k \int_{x \in \omega_k} \left| \fint_{x' \in \omega_k} u(x') \mathrm{d}x' - u(x) \right|^2 \mathrm{d}x \right)^{\frac{1}{2}} \\
&\leq \left(\sum_k \int_{\omega_k} \left(\underbrace{\sqrt{\operatorname{diam}(\omega_k)}}_{\leq \sqrt{h}} \, \|u'\|_{L^2(\omega_k)} \right)^2 \mathrm{d}x \right)^{\frac{1}{2}} \\
&\leq \sqrt{h} \left(\sum_k \underbrace{\operatorname{vol}(\omega_k}_{\leq h} \, \|u'\|^2_{L^2(\omega_k)} \right)^{\frac{1}{2}} \qquad (8.1) \\
&\leq h \|u'\|_{L^2(\Omega)}. \qquad (8.3)
\end{aligned}$$

The $L^2(\Omega)$-norm of $\partial_x \rho \mathcal{B} u$ can be estimated by the $L^2(\Omega)$-norm of u by expanding u in a Fourier series and estimating the coefficients of $\partial_x \rho \mathcal{B} u$. Since $\rho\mathcal{B}$ is self–adjoint, the supremum of the modulus of the spectrum of $\partial_x \rho \mathcal{B}$ is the operator norm in $\mathrm{Lin}(L^2(\Omega), L^2(\Omega))$. Hence $\|\partial_x \rho \mathcal{B}\| \leq \sup_{k \in \mathbb{R}} \frac{\rho \pi k}{\rho + k^2 \pi^2} = \sqrt{\frac{\rho}{2}}$. By estimate (8.2), the inequality $\|(Id - \pi_h)\rho\mathcal{B}\|_{\mathrm{Lin}(L^2(\Omega), L^2(\Omega))} \leq Ch$ where $C = \sqrt{\frac{\rho}{2}}$ is established. Repeating the last step gives us the desired estimate $\|(Id - \pi_h)\rho\mathcal{B}\|_{\mathrm{Lin}(L^2(\Omega), L^2(\Omega))} \leq Ch^2$.

Stability

The next step is to control $d_2(\Psi_0, \Psi(t))$ using Gronwall's inequality. This result is a purely analytical estimate for the exact system (4.2).

$$\begin{aligned}
&\left\| \langle \Psi_0(y), |\phi_t(y) - y| \rangle_{y \in \mathbb{R}^2} \right\|_{L^2(\Omega)} \\
= &\left\| \left\langle \Psi_0(y), \left| \int_0^t \begin{pmatrix} \phi_{s,2}(y) - y_2 + y_2 \\ -\sigma \circ \phi_{s,1}(y) + \rho \mathcal{B} \langle \Psi_0, \sigma \circ \phi_{s,1} \rangle \end{pmatrix} \mathrm{d}s \right| \right\rangle_{y \in R^2} \right\|_{L^2(\Omega)} \\
\leq &\int_0^t \left(\ell + \|\rho\mathcal{B}\| \|\sigma'\|_{L^\infty(\mathbb{R})} \right) \cdot \| \langle \Psi_0(y), |\phi_s(y) - y| \rangle \| \mathrm{d}s \\
+ &\int_0^t \| \langle \Psi_0(y), | -\sigma(y_2) + \sigma_0 + \rho\mathcal{B} \langle \Psi_0(d\widetilde{y}), \sigma(\widetilde{y}_2) - \sigma_0 \rangle | \rangle \|_{L^2(\Omega)} \mathrm{d}s + t\sigma_0(1 + \|\rho\mathcal{B}\|) \\
\Rightarrow \quad &\| \langle \Psi_0(y), |\phi_t(y) - y| \rangle \|_{L^2(\Omega)} \leq \widetilde{C} e^{\left(2\ell + \|\rho\mathcal{B}\| \, \|\sigma'\|_{L^\infty(\mathbb{R})} \right) t}, \qquad (8.3)
\end{aligned}$$

where $\widetilde{C} = (1 + \|\rho\mathcal{B}\|)\left(\|\sigma'\|_{L^\infty(\mathbb{R})}\,\langle\Psi_0(y), |y|\rangle + \sigma_0\right)$ and $\sigma_0 = |\sigma(0)|$. Using this, we can estimate the error due to the discretization:

$$\begin{aligned}
d_2(\Psi(t), \Psi^{h,N}(t)) &= \left\| \sup_{\mathrm{lip}(g)\le 1} \langle \Psi_0, g\circ\phi_t - g\circ\phi_t^h\rangle \right\|_{L^2(\Omega)} \le \left\| \left\langle \Psi_0, \left|\phi_t - \phi_t^h\right|\right\rangle \right\|_{L^2(\Omega)} \\
&\le \int_0^t \left\| \left\langle \Psi_0, \begin{pmatrix} \phi_{s,2} - \phi_{s,2}^h \\ -\sigma\circ\phi_{s,1} + \sigma\circ\phi_{s,1}^h \end{pmatrix} \right\rangle \right\|_{L^2(\Omega)} \\
&+ \left\| \rho\mathcal{B}\langle\Psi_0, \sigma\circ\phi_{s,1}\rangle - \pi_h\rho\mathcal{B}\langle\Psi_0, \sigma\circ\phi_{s,1}^h\rangle \right\|_{L^2(\Omega)} \mathrm{d}s \\
&\le \int_0^t \ell \left\| \left\langle \Psi_0, \left|\phi_s - \phi_s^h\right|\right\rangle \right\|_{L^2(\Omega)} \\
&+ \|(Id - \pi_h)\rho\mathcal{B}\| \,\|\, \langle\Psi_0, \sigma\circ\phi_{s,1}\rangle \,\|_{L^2(\Omega)} \\
&+ \|\pi_h\rho\mathcal{B}\| \,\|\langle\Psi_0, |\sigma\circ\phi_{s,1} - \sigma\circ\phi_{s,1}^h|\rangle\|_{L^2(\Omega)}\, \mathrm{d}s.
\end{aligned}$$

The second term can be controlled using the stability inequality (8.3)

$$\begin{aligned}
\|\langle\Psi_0, \sigma\circ\phi_{t,1}\rangle\| &\le \|\,\langle\Psi_0, |\sigma\circ\phi_{t,1} - \sigma|\rangle\,\| + \|\,\langle\Psi_0, \sigma\rangle\,\| \\
&\le \|\sigma'\|_{L^\infty(\mathbb{R})}\left(\|\,\langle\Psi_0(y), |\phi_t(y) - y|\rangle\,\| + \|\langle\Psi_0(y), |y|\rangle\,\|_{L^2(\Omega)}\right) + \sigma_0 \\
&\le \|\sigma'\|_{L^\infty(\mathbb{R})}\,\widetilde{C}e^{(2\ell + \|\rho\mathcal{B}\|\,\|\sigma'\|_{L^\infty(\mathbb{R})})t} + \|\sigma'\|_{L^\infty(\mathbb{R})}\,\langle\Psi_0(y), |y|\rangle + \sigma_0.
\end{aligned}$$

Using Gronwall's inequality again, one gets

$$\begin{aligned}
& d_2(\Psi(t), \Psi^{h,N}(t)) \\
\le\ & Ch^2 e^{\left(\ell + \|\sigma'\|_{L^\infty(\mathbb{R})}\|\rho\mathcal{B}\|\right)t} \cdot \left\{ \widetilde{C}e^{\left(2\ell + \|\rho\mathcal{B}\|\,\|\sigma'\|_{L^\infty(\mathbb{R})}\right)t} + \|\sigma'\|_{L^\infty(\mathbb{R})}\,\langle\Psi_0(y), |y|\rangle + \sigma_0 \right\}.
\end{aligned}$$

Setting $\widetilde{\widetilde{C}} := C(\|\sigma'\|_{L^\infty(\mathbb{R})}\,\widetilde{C} + \|\sigma'\|_{L^\infty(\mathbb{R})}\,\langle\Psi_0(y), |y|\rangle + \sigma_0)$ yields the desired estimate

$$d_2(\Psi(t)), \Psi^{h,N}(t)) \le \widetilde{\widetilde{C}}he^{3(\ell + \|\sigma'\|_{L^\infty(\mathbb{R})}\|\rho\mathcal{B}\|)t}.$$

□

Acknowledgments. F. T. wishes to thank Professor Alexander Mielke for his constant encouragement and many helpful suggestions. He is also grateful to Professor Felix Otto and Professor G. Maugin for helpful comments. V.I.L. acknowledges discussions with Professor Erwin Stein. The support of the VW-Foundation under the project I/70 284 and I/70 282 "Stress and strain induced phase transformations in engineering materials" at the University of Hannover, Germany, is greatly acknowledged. Both authors thank the referee for enlightening comments.

REFERENCES

[1] Levitas, V. I.: Post-bifurcation behavior in finite elastoplasticity. Applications to strain localization and phase transitions, Universität Hannover. Institut für Baumechanik und Numerische Mechanik, *IBNM-Bericht 92/5*, 1992a.

[2] Levitas, V. I., Stein, E., and Lengnick, M.: On a unified approach for the description of phase transitions and strain localization. *Arch. Appl. Mech.*, **66**, 242-254 (1996).

[3] Levitas, V. I.: On mechanics-thermodynamics analogy and inertia of thermodynamic processes. *Doklady AN Ukrainskoi SSR*, Ser. A, vol 10, 39-46 (1981).

[4] Levitas, V. I.: *Thermomechanics of Phase Transformations and Inelastic Deformations in Microinhomogeneous Materials*, Naukova Dumka, Kiev, 1992.

[5] Levitas, V. I.: Plasticity theory of microinhomogeneous materials at large strain gradient. *Mechanics Research Communications*, **21**(1), 11-17 (1994).

[6] Slemrod, M.: A limiting "viscosity" approach to the Riemann problem for materials exhibiting change of phase. *Arch. Rat. Mech. Anal.*, **81**, 327-365 (1989).

[7] Abeyaratne, R. and Knowles, J. K.: Kinetic relations and the propagation of phase boundaries in solids. *Arch. Rat. Mech. Anal.*, **114**, 119-134 (1991).

[8] Truskinovsky, L.: Transition to detonation in dynamic phase changes. *Arch. Rat. Mech. Anal.*, **125**, 375-397 (1994).

[9] Abeyaratne, R. and Knowles, J. K.: Implications of viscosity and strain-gradient effects for the kinetics of propagating phase boundaries in solids. *SIAM J. Appl. Math.,* **5**, 1205-1221 (1991).

[10] Ball, J. M. and James, R. D.: Fine phase mixtures as minimizers of energy. *Arch. Rat. Mech. Anal.*, **100**, 13-52 (1987).

[11] Tartar, L.: Solutions oscillantes des equations de Carleman. *Seminaire Goulaouic–Meyer–Schwartz 1980-1981*, Ecole Polytechnique (Palaiseau). Expose XII, 1981.

[12] Tartar, L.: Oscillations and asymptotic behaviour of two semilinear hyperbolic systems, in *Dynamics of Infinite Dimensional Systems*, pp. 341-356, ed. S. N. Chow and J. K. Hale, Springer-Verlag, New York (1987).

[13] Tartar, L.: Oscillations for semilinear systems. Unpublished lecture notes, no. 91.3, 1991, 14 pp.

[14] Kinderlehrer, D., and Pedregal, P.: Weak convergence of integrands and the Young measure representation. *SIAM J. Math. Anal.*, **23**(1), 1-19 (1992).

[15] Theil, F.: Young-measure solutions for a viscoelastically damped wave equation with nonmonotone stress-strain relation. *Arch. Rat. Mech. Anal.*, **144**, 47-78 (1998).

[16] Batt, J., Morrison, P. J., and Rein, G.: Linear stability of stationary solutions of the Vlasov-Poisson System in three dimensions. *Arch. Rat. Mech. Anal.*, **130**, 163-182 (1995).

[17] Jordan, R.: A statistical equilibrium model of coherent structures in magneto hydrodynamics. *Nonlinearity*, **8**, 585-613 (1995), Corrigendum *Nonlinearity*, **8**, 1207 (1995).

[18] Jordan, R. and Turkington, B.: Maximum entropy states and coherent structures in magneto hydrodynamics, in *Maximum Entropy and Bayesian Methods*, pp. 374-353, ed. K. M. Hanson and R. N. Silver, Kluwer Academic, New York, 1996.

[19] Fermi, E., Pasta, J., and Ulam, S.: Studies of nonlinear problems. *Los Alamos Technical Reports, Document LA-1940*, 1955.

[20] Love, A.E.H.: *A Treatise on the Mathematical Theory of Elasticity*, Cambridge University Press, Cambridge, UK, 1927; Dover, New York, 1944.

[21] Bogolubsky, I. L.: Some examples of inelastic soliton interaction. *Comp. Phys. Comm.*, **13**, 149-155 (1976).

[22] Boussinesq, M. J.: Théorie des ondes et de remous qui se propagent le long d'un canal rectangulaire horizontal, en communiquant au liquide contenu dans ce canal des vitesses sensiblement pareilles de la surface au fond. *J. Math. Pures Appl. (Ser. 2)*, **17**, 55-108 (1872).

[23] Soerensen, M. P., Christiansen, P. L., and Lomdahl, P. S.: Solitary waves on nonlinear elastic rods I. *J. Acous. Soc. Am.*, **76**(3), 871-879 (1984).

[24] Rosenau, P.: Dynamics of dense lattices. *Phys. Rev. B*, **36**(11), 5868-5876 (1987).

[25] Valanis, K. C.: Irreversible thermodynamics with internal inertia. Principle of stationary total dissipation. *Arch. Mech.*, **24**(5–6), 849-862 (1972).

[26] Clarkson, A., LeVeque, R. J., and Saxton, R.: Solitary-wave interactions in elastic rods. *Stud. App. Math*, **75**, 95-122 (1986).

[27] Abeyaratne, R. and Knowles, J. K.: On the dissipative response due to discontinuous strains in bars of unstable elastic material. *Int. J. Solids Structures*, **24**, 1021-1044 (1988).

[28] Levitas, V. I.: Thermomechanical description of pseudoelasticity - The threshold–type dissipative force with discrete memory. *Mech. Res. Commun.*, **21**, 273-280 (1994).

[29] Fu, S., Huo, Y., and Müller, I. M.: Thermodynamics of pseudoelasticity: An analytical approach. *Acta Mechanica*, **99**, 1-19 (1993).

[30] Theil, F.: *Young-Measure Solutions for Nonlinear Partial Differential Equations* (in German), Dissertation, Universität Hannover, Germany, 1997.

[31] Theil, F.: Young-measure solutions for a microkinetically regularized wave equation. In preparation, 1998.

[32] Mielke, A.: Flow properties for Young–measure solutions of semilinear hyperbolic problems. *Proc. Roy. Soc. Edin.*, **129A**, 85-123 (1998).

[33] Roubicek, T.: *Relaxation in Optimization Theory and Variational Calculus*, De Gruyter, New York, 1997.

[34] Rachev, S. T.: *Probability Metrics and the Stability of Stochastic Models*, John Wiley, New York, 1991.

[35] Reich, S.: *Dynamical Systems, Numerical Integration, and Exponentially Small Estimates*, Habilitationsschrift, FU Berlin, 1997.